Influence of Dynamic River Stage on The Vulnerability of Water Wells and Structure Foundations in Cold Regions

by

Haoyu Yin

A thesis

presented to the University of Waterloo

in fulfillment of the

thesis requirement for the degree of

Master of Science

in

Earth Sciences

Waterloo, Ontario, Canada, 2023

Author's Declaration

I hereby declare that I am the sole author of this thesis. This is a true copy of the thesis, including any required final revisions, as accepted by my examiners.

I understand that my thesis may be made electronically available to the public.

Abstract

Groundwater is important for people in Northern Canada, yet the groundwater protection protocols and water well vulnerability assessments designed for other warmer regions of Canada may not be applicable to communities in Northern Canada due to the unique hydrogeological characteristics there. The seasonal melt of snow and ice leads to intense river stage fluctuations and might cause flooding issues for the adjacent floodplain; however, their influences on the vulnerability of drinking water wells and nearby infrastructure are not fully understood. This research considers a case study at Carmacks, central Yukon, where an integrated surface-subsurface numerical modelling code was used to examine these processes. The model results indicate that the annual variation in the river stage temporarily reverses the direction of the hydraulic gradient between the surface water body and the adjacent aquifer. Stream reaches that gain groundwater under lower river stages can become losing streams during the high stage periods, which facilitates the transport of solute from the river to the adjacent aquifer. Additionally, the model shows that the annual river stage variation can temporarily alter the size and orientation of the region that contributes water to pumping wells, which means new environmental threats could become important. In terms of travel time, the model results suggest that annual river stage variation accelerates the transport of river-origin solutes to the adjacent aquifer, and higher river peaks facilitate more rapid solute migration. Thus, the natural protection of the soil travel path against microbial pathogens may become inefficient and water wells may become more vulnerable. The model results also demonstrate that higher peak river stages are more likely to cause basement inundation in buildings on the riverbank than average peaks, and that the duration of basement inundation varies at different locations.

Acknowledgements

First of all, I would like to express my sincere appreciation to my supervisor Dr. Dave Rudolph who offered me the opportunity three years ago and has always been inspiring, guiding and encouraging me since the moment I started my master's program at the University of Waterloo with patience and expertise in groundwater research. Dr. Dave Rudolph is not only a mentor but also a close friend of mine with whom I can share academic ideas and daily life. It is my greatest pleasure working with Dr. Dave Rudolph, and I hope there is a chance for me to work with him again in the future.

I would like to express my deep appreciation to Dr. Andrew Wiebe for all the kind help and guidance for my research project. As one of my committee members, Dr. Andrew Wiebe's detailed instructions and smart ideas are crucial for my numerical model construction and thesis writing. I also appreciate the encouragement whenever I meet new challenges and feel lost during my program.

I also want to extend my true thanks to my other committee members: Dr. Jeffrey McKenzie from McGill University and Dr. Walter Illman from the University of Waterloo. I would like to thank Dr. Jeffery McKenzie for the research ideas in the initial project proposal and for all the kind help during this research program. I would like to thank Dr. Walter Illman for giving me great suggestions about numerical model boundary selection and boundary conditions during the course of my research.

I would also like to express my special appreciation to Professor Young Jin Park and Rob McLaren for their extensive professional assistance and guidance in building and debugging the numerical model and for solving technical problems. Their knowledge of simulating groundwater-surface water flow and solute transport using the numerical model is key for the entire project.

I also appreciate the support from the Little Salmon Carmacks First Nation and Village of Carmacks, as well as the assistance and advice from Brendan Mulligan from the Water Resources Branch of Yukon Government.

I am also grateful for the help and friendship from my colleagues in the office PHYS229 who are Brampton Dakin, Chenxi Wang, Corey Zanatta, Jiangyue (Joey) Ju, Jiaqi Weng, Matthew Pendleton, Ning Luo, Oliver Conway-White, Xin Tong, and Zeren Ning.

Finally, I would like to show my deepest gratitude to my loved parents and family who support me whatever happens. I would also like to thank Jane Wang for all her love and support.

Founding for this research was provided by Engineering Research Council of Canada (NSERC), the Government of Yukon, and Global Water Futures (GWF).

Table of Contents

List of Figures

Chapter 1
Introduction

1.1 Background

Groundwater is an important freshwater source for people living in Northern Canada. The cold environment and freezing conditions in Northern Canada during winter limit access to surface water, making groundwater a more sustainable water source for year-round usage. For example, Statistics Canada (2021) claims that in 2019 among all the Yukon residents served by drinking water plants, over 98% relied on groundwater as the water source. Meanwhile, many communities in Northern Canada are established near rivers and streams and are underlain by permeable sediments such as fluvial and alluvial sediments. Their water supply systems may be hydraulically connected to the surrounding surface water bodies. The presence of contaminants and microbial pathogens in surface water bodies could lead to negative impacts on groundwater quality; therefore, weighing the vulnerability of groundwater aquifers and water wells against the potential impacts of these threats should be assessed in Northern Canada to protect drinking water sources.

In Northern Canada, snow and ice melt during the early spring and summer seasons, leading to intense runoff events and causing seasonal river stage variation. As many communities are located near rivers and have municipal and domestic water wells constructed within shallow unconfined aquifers that are hydraulically connected to the surrounding rivers, the fluctuation in the river stage could influence the vulnerability of these water wells. However, to our best knowledge, no standard vulnerability assessment approaches have been recommended for Northern Canada that consider the impacts of seasonal river stage and flooding. In addition, the rise of the river stage could induce an elevated water table and cause basement inundation issues for houses located at the riverbank.

1.2 Objectives

The main goal of this thesis is to examine the influences of seasonal river stage variation on the vulnerability of water wells and household infrastructure in cold regions. This thesis presents a case study at the community of Carmacks, Yukon, where the vulnerability of the public water supply well and the basement inundation issues were evaluated using a numerical modelling approach, and multiple simulation scenarios were designed to examine the impacts of annual river stage variation. This case study aims to improve the understanding of the influences of seasonal river stage variation

on 1) the vulnerability of water supply wells constructed within a river-connected aquifer and 2) household basements located near the fluctuated river.

1.3 Thesis organization

There are three chapters in this thesis. Chapter 1 introduces the general background and main objectives of the thesis. Chapter 1 is followed by Chapter 2, which is written in manuscript format and ready for submission to scientific journals. Chapter 3 concludes the thesis and includes recommendations for future research.

Chapter 2
Influence of Dynamic River Stage on The Vulnerability of Water Wells and Structure Foundations in Cold Regions

2.1 Introduction

Groundwater as a freshwater source is important to people living in Yukon, Canada. Statistics Canada (2021) claims that in 2019 among all the Yukon residents served by drinking water plants, over 98% relied on groundwater as the water source. The cold environment and freezing conditions during winter limit access to surface water, making groundwater a more sustainable water source for year-round usage. Many communities in the Yukon, Canada, are underlain by alluvial, fluvial, and glaciofluvial sediments (Tetra Tech, 2017b), which also facilitates the utilization of groundwater resources. However, many water supply systems are located near rivers and streams and have their water wells constructed within unconfined aquifers (Tetra Tech, 2017b) that may be hydraulically connected to adjacent surface water bodies. The presence of contaminants and microbial pathogens in rivers could lead to different degrees of negative impacts on groundwater quality, depending on the chemical behaviour of the contaminants, the relative position of the contaminant with respect to a receptor (e.g., a pumping well), and the physical protective functions of flow paths. Weighing the vulnerability of groundwater sources against the potential impacts of the river-originated threats should be assessed to develop a sustainable regional groundwater supply in Yukon, Canada.

Many vulnerability assessment tools and groundwater protection protocols were designed for southern regions (warmer climates). However, in Yukon, many water supply systems are located close to rivers and are subject to seasonal river stage variations caused by snow and ice melt, which might affect the water wells and makes vulnerability assessment and groundwater protection different from southern Canada. The strong fluctuation of the river stage induces a transient groundwater flow field, which can reorient the well capture zone (Rayne et al., 2014) and may affect solute transport. To our best knowledge, no standard vulnerability assessment approaches have been recommended for northern Canada that consider the impacts of seasonal river stage and flooding. In addition to well vulnerability, the rise of the river stage can quickly propagate to the adjacent river-connected aquifer and elevate the water table. In Yukon, many communities are established near rivers; therefore,

household basement inundation issues induced by the high water table could affect many Yukon residents.

This document presents a case study at the community of Carmacks, Yukon. At the study site, a municipal water supply well is constructed within an unconfined aquifer that is hydraulically connected to the adjacent Yukon River, which had more than 4 meters of seasonal river stage fluctuation during 2021 and 2022. The vulnerability of the water supply well was evaluated using a numerical modelling approach, and multiple simulation scenarios were designed to examine the impacts of annual river stage variation. The risk, timing, and duration of basement inundation at the study site were also analyzed. This study aims to improve the understanding of well vulnerability in cold regions where the river stage seasonally fluctuates and to demonstrate the application of numerical modelling in riverbank infrastructure damage analysis.

2.2 Background

2.2.1 River-Connected Aquifer Systems

In the current study, the concept of a river-connected aquifer refers to a hydrogeologic system consisting of river channels embedded within fluvial or alluvial derived deposits that are permeable and capable of storing and transmitting groundwater. An important feature of a river-connected aquifer is that groundwater in the shallow aquifer materials may directly interact with surface water in the river, which is induced by the hydraulic gradient between the water table and the river stage. Woessner (2000) classified the interactions into four types: 1) gaining, when groundwater flows into a river; 2) losing, when a river is replenishing the groundwater system; 3) flow-through, when the river channel receives groundwater on one side but also loses water to the groundwater system on the other side; and 4) parallel, when the groundwater and the river have a same flow direction without exchanging water. Among these various river-streambank interactions, flow-through interactions generally occur when a stream reach cuts across a groundwater flow direction that is the same on both sides of the stream, which results groundwater flow through the channel from the upgradient side to the downgradient side (Fetter, 2001). The other three types of interactions are more likely to happen when the general orientation of the stream reach and the average valley or fluvial plain slope directions are nearly parallel (Woessner, 2000).

In addition to natural river-connected aquifer interactions, anthropogenic activities such as water well pumping can also introduce or alter the interactions. Pumping from a river-connected aquifer may not only withdraw local groundwater from aquifer sediments around the well screen but also induce surface water to flow from the river towards the well. While providing an important component of recharge to supply the pumped aquifer, river water entering the shallow groundwater system can also lead to water quality issues in adjacent wells (Winter et al., 1998). For example, a case study by Duncan et al. (1991) at a well field along the Platte River in east-central Nebraska demonstrated that atrazine, a type of herbicide, contained in the river could be transported to wells through recharge induced by pumping. Therefore, a groundwater protection plan such as a well vulnerability assessment may be necessary for water supply wells that are constructed in river-connected aquifer systems. However, the unique characteristics of river-connected aquifer systems require special consideration when developing aquifer and well protection plans and some of the main concepts and considerations are discussed below.

2.2.2 Aquifer and Well Vulnerability in River-Connected Aquifer Systems

A well capture zone is a three-dimensional subsurface region that contributes groundwater to a well. Because the water table in most real cases is not perfectly flat and there exists a regional hydraulic gradient, the capture zone may not form a symmetrical cylinder around the pumping well but may take a more elliptical shape over a larger region extending in the up-gradient direction. A well capture zone is formed once pumping starts and keeps growing until it reaches a steady state where the aquifer recharge flux equals the extraction rate. The steady-state well capture zone can be divided into time-of-travel (TOT) zones that reflect the time groundwater takes to travel from its original position within the aquifer to the well screen. The steady-state well capture zone is often divided into TOT zones of 150 days to 250 days, 5 years, and 25 years for analyzing bacterial contaminants, petroleum products, and chlorinated solvents, respectively (Frind et al., 2006). Wells are classified as being under the direct influence of surface water (GUDI) if the TOT is estimated to be 50 days or less (Ontario Ministry of the Environment, Conservation, and Parks [OMECP], 2016).

GUDI refers to a situation where microbial pathogens and other contaminants in the surface water body fail to be filtered and attenuated by subsurface material prior to arrival at the extraction point and are thus captured by a water supply well. For a water supply well under GUDI conditions, conventional groundwater treatment may be insufficient to produce safe drinking water; therefore,

more stringent disinfection processes are required (Chin & Qi, 2000). A 50-day TOT from the surface water body to the well screen can be used to evaluate the potential for a well of concern to experience GUDI conditions since microbial pathogens are often assumed to be inactivated after this threshold time (Chaudhary et al., 2009; Frind et al., 2002; OMECP, 2016; Wiebe et al., 2021). As such, delineating the 50-day TOT for a drinking water well may be useful in river-connected aquifer systems where groundwater and water supply wells are suspected to be vulnerable to exposure to microbial pathogens originating from river waters.

2.2.3 Groundwater Protection Strategies

The conventional approach for groundwater protection is based on a wellhead protection area (WHPA), which is determined according to the time contaminants within the well capture zone travel within the saturated subsurface before being captured by the well. The WHPA is divided into different TOT zones to analyze the risks of various types of contaminants which would cease to be harmful or become inactivated after a certain amount of time. However, some organic compounds such as chlorinated solvents may persist in groundwater for many decades (Eberhardt & Grathwohl, 2002, Frind et al. 2006), making it possible for them to be captured by a well from anywhere within the capture zone. Therefore, the entire capture zone should be considered for a comprehensive protection plan (Vassolo et al., 1998).

Methods for delineating well capture zones include analytical solutions and numerical modelling. The advantages of numerical modelling over analytical solutions are the capabilities of representing complex hydrogeological settings and groundwater-surface water interactions, leading to more accurate capture zone delineation results (Frind et al., 2002). A common workflow of the numerical modelling approach is solving for the steady-state flow field first, then incorporating a backward particle tracking algorithm which places numerical "*particles*" at the well screen and calculates the travel path of these particles over time away from the well based on advective flow. A particle tracking algorithm can be incorporated within conventional numerical models such as WATFLOW (Frind et al., 2002), MODFLOW (Barry et al., 2009; Dong et al., 2013) and FEFLOW (Diersch, 2014). However, the particle tracking approach does not usually consider dispersion, also known as hydrodynamic dispersion, which is an important process in solute transport (Frind et al., 2006). Without considering the dispersion process, particle tracking might produce a smaller well capture zone and miss possible contaminant sources of relevance.

According to Vrba and Zoporozec (1994), aquifer “vulnerability” refers to a fundamental property of a groundwater system which reflects how sensitive the system is to human and natural impacts. They also introduced the concepts of "intrinsic vulnerability," which is solely related to hydrogeological factors, and "specific vulnerability," in which the impacts of contaminants and land use are additionally considered. In the paper by Frind et al. (2006), the definitions of intrinsic vulnerability and specific vulnerability are further explained and distinguished: intrinsic vulnerability describes the protective function that a natural hydrogeologic system can give to the groundwater without taking the characteristics of the contaminants into account, while specific vulnerability furthermore considers the chemical properties of the contaminants. In addition, they also introduced the use of prefixes "aquifer" and "well" to clearly represent the research targets; for instance, "intrinsic aquifer vulnerability" represents that the research interest is the protective function of the overlaying layers above the aquifer; whereas "intrinsic well vulnerability" should be used when the research interest is the protective function of the entire flow path from the contaminant source to the receptor well. Following their work, the term “well vulnerability” used in the current work includes both the intrinsic and the specific components.

Common aquifer/well vulnerability assessment methods can be classified into three main categories: (1) Index/Overlay methods, (2) Statistics-based methods, and (3) Process-based methods. In the Index/Overlay methods, ranking or numerical scores are assigned to the study area based on attributes including geology, soil texture, depth to the water table, and the location of the surface contaminants. Ranking or a numerical score for each attribute over the study area can be treated as an independent layer, and multiple layers can be imported into GIS software and overlaid to produce an overall vulnerability map. One example of the Index method is the DRASTIC method (Aller et al., 1987). Although an Index method is a simple and relatively easy approach to conducting an aquifer/well vulnerability assessment, it requires subjective judgment and rating, potentially making it unreliable and non-unique (Frind et al., 2006; Liggett & Talwar, 2009).

Statistics-based methods analyze various types of information such as geology, well depth, and land use with regression models and calculate the probability that the contaminant concentration exceeds a drinking water limit rather than ranking the vulnerability level to high, medium, or low (Liggett & Talwar, 2009; Focazio et al., 2002). Statistics-based methods objectively evaluate the influences of potential factors such as soil type, well depth, and fertilizer applications on vulnerability (Focazio et al., 2002), and are easier to use than Process-based methods, which typically require

detailed stratigraphic information. However, Statistics-based methods lack the ability to fully account for the complexity of groundwater flow processes (Focazio et al., 2002). Also, in many cases, there is not enough information available to conduct a viable statistical analysis.

The hydrogeologic Process-based methods simulate the processes governing groundwater flow and sometimes contaminant transport, utilizing various types of models. These range from simple analytical models to complex numerical models in 2D and 3D. Even though the Process-based methods are powerful, they can be complicated and laborious to implement, especially when the target study area is spatially large; however, this is considered an ideal approach for assessing well vulnerability at the local scale (Focazio et al., 2002).

Frind et al. (2006) introduced an alternative approach to particle tracking within Process-based models to more completely evaluate well vulnerability through the use of a novel solute transport modeling approach. Their study demonstrated the idea of using forward/backward solute transport models for well vulnerability assessment and emphasized critical information that should be extracted from the model: 1) the time taken for concentration to breach a threshold level, 2) the maximum concentration and time taken to reach it, and 3) the duration of above-threshold concentrations at the well. They clarified that the forward transport model approach is straightforward but would be impractical for a large target study area with many potential contaminant sources, whereas the backward transport model, which tracks solute transport in the reverse direction (away from the receptor(s)), would be a more efficient tool for dealing with a large-scale problem. But the forward transport model needs to be completed at least once to generate a breakthrough curve to which the backward model can be compared to calculate a scale factor for calibration purposes. Both the forward and backward transport model in their research were simulated under a steady-state flow field.

2.2.4 Unique Characteristics of River-Connected Aquifer Systems

The dynamics of river stage can affect water exchange between rivers and streambanks. Winter et al. (1998) described that a sudden rise of river stage can cause water to flow from the river into its adjacent riverbanks, a process called bank storage, which tends to buffer increases in streamflow. They also pointed out that water lost to the riverbanks during the bank storage process partially flows back into rivers within a certain time period ranging from days to years after the river stage drops.

Also, the dynamics of the river stage and related flooding issues are believed to threaten groundwater quality. Derx et al. (2013) analyzed virus transportation under flooding events in a river-connected aquifer using a coupled groundwater-surface water model. Their simulation results indicated that compared with a non-flooding scenario, the elevated river stage enables the virus contained in a river to travel further into the streambanks with a higher detected concentration in groundwater. In addition to the water exchange that happens at the river-streambanks interface, overbank flooding can also take place when the elevated river stage overtops the streambanks, and water in the flooded area recharges the water table (Winter et al., 1998). Similar to a temporary surface water body induced by snowmelt and/or heavy rain that may increase the vulnerability of a nearby water supply well (Wiebe et al., 2021), overbank flooding that flows through and covers large areas of the land surface might also threaten the water quality of a well field.

In addition to the water quality concerns, the rising of the river stage can also cause basement inundation problems for people who live near the flooded river. According to a study conducted in the City of Calgary, Canada, by Abboud et al. (2017), recharge from the flooded river to the adjacent aquifer elevated the water table and was the primary reason for basement inundation issues in the study area.

Because a river plays an important role in a river-connected aquifer, the characteristics of rivers in Northern Canada with a cold climate need to be reviewed. Brabets et al. (2000) discussed relevant hydrologic characteristics of the Yukon River Basin and stated that the average historical flow rate data of the Yukon River and its major tributaries tend to have greater streamflow from May to September compared with other months during a year. This greater flow is induced by rainfall, snowmelt, ice melt, and glacier ice melt. These authors also pointed out that ice jams during the spring season are the main cause of flooding in the Yukon River. For example, in a more recent study on flooding processes of major rivers in Yukon, Canada, it was suggested that the river ice breakup and associated ice jams can be a common cause for flooding in communities including Old Crow and Dawson; however, some communities such as Mayo, Pelly Crossing, and Carmacks are subject to flooding that is mainly induced by spring snowmelt and associated high river discharge (Turcotte, 2021). These unique characteristics of Northern rivers can draw water quality concerns. For example, bacteria were detected at water supply wells that were constructed within a river-connected aquifer in the community of Dawson, which might be induced by the high bacterial load in adjacent rivers during the river ice breakup period in early spring (Tetra Tech, 2017a). They also suggested that the

detection of bacteria in the water supply wells tends to closely relate to the occurrence of the spring freshet and rise of river levels.

2.3 Methodology

2.3.1 Study Site

The study site for the current research is the community of Carmacks (Carmacks), which is located at the confluence of the Yukon River and the Nordenskiold River in Central Yukon (Fig. 1). Carmacks covers approximately $43 km^2$ and has about 500 residents living at the Village of Carmacks and the adjacent Little Salmon/Carmacks First Nation (LS/CFN) settlement lands. Part of the LS/CFN settlement is located on a point bar that is nearly surrounded by the Yukon River. The drinking water supply for LS/CFN residents is derived from a public supply well (PW-05) located on the point bar and the raw water is treated at a water treatment plant and distributed to residents through a trucked drinking water distribution system and a pipeline system (Morrison Hershfield, 2020). In addition to PW-05, Carmacks has many domestic wells screened in the shallow aquifer for private household usage. Detailed information about the domestic wells that have been registered can be found on the Yukon Water Well Registry website (https://yukon.maps.arcgis.com/apps/webappviewer/index.html?id=51322dfb133d42c4ad184fee9986048b). The locations of the water treatment plant (PW-05 well) and other registered domestic wells are indicated in Fig. 2.

The Yukon River flows through the community from the east (upstream direction) to northwest (downstream direction), with water from the Nordenskiold River entering into the Yukon River at a meander within the community. The levels of the Yukon River at Carmacks show seasonal variations, as can be noticed from Fig. 3. The short-term river stage variation during early spring (the month of April) and early winter (the months of November and December) are interpreted to be induced by the breakup of ice cover of the Yukon River in the upstream direction and the formation of ice in Yukon River, respectively (Turcotte, 2021). In addition, the river has a stronger stage variation during late spring and summer (between May and August), which is interpreted to be induced by increased river flow rates due to snow melt and precipitation events (Turcotte, 2021). The historical data also demonstrate that the variation in river stage during spring and summer has become more intense and the highest level of the Yukon River stage is increasing in recent years (2021 and 2022), as compared

to the past years (from 2015 to 2020). Potential contaminants contained in the Yukon River at Carmacks include petroleum hydrocarbons as the result of the spilling of hydrocarbon within the community (Morrison Hershfield, 2020) and potential bacterial pathogens associated with the release of raw sewage at various locations along the river (Erwin, 2023; Henney, 2022).

Fig. 4 shows the locations of two cross-section diagrams (A-A' and B-B') that demonstrate the stratigraphy of Carmacks, and Fig. 5 illustrates the cross-section diagrams. The cross-section diagrams were drawn based on data from the aquifer mapping report from Golder Associates (2021). According to the report, the surficial sediments are mainly made up of glaciofluvial deposits, fluvial deposits, eolian deposits, and colluvial deposits. These deposited materials correspond to two identified aquifers, referred to as the shallow Chu Íntthi and deeper Łots'an Aquifers. Both are unconfined aquifers with a similar composition of sand and gravel, but the Chu Íntthi Aquifer is associated with fluvial deposition of the Yukon River and the Nordenskiold River whereas the Łots'an aquifer is interpreted to have formed during the end of last glaciation period. The two aquifer units are in direct hydraulic connection. Golder Associates (2021) also states that the domestic wells are drilled within the shallow Chu Íntthi Aquifer, whereas the PW-05 public supply well was identified to be screened within the deeper Łots'an Aquifer. While the two aquifers overlay the assumed impermeable Carmacks Aquitard, another potential aquifer consisting of gravel and sand may exist at the bottom of the unconsolidated sediment sequence, based on one borehole log; however, there is insufficient borehole data to delineate this unit confidently on a map (Fig. 5).

Underlying the inferred aquifers is bedrock that has been classified into the following three groups: (1) the Upper Cretaceous Carmacks Formation, which is comprised of augite-olivine basalt and breccia; (2) the Upper Jurassic and Lower Cretaceous Tantalus Formation, which is comprised of chert pebble conglomerate and gritty quartz-chert-feldspar sandstone; and (3) the Lower and Middle Jurassic Tanglefoot Formation, which is comprised of arkosic sandstone and minor shale, pebble and boulder conglomerate (Yukon Geological Survey, 2022).

The study site also contains a glacial deposit called the McConnell Ice Stagnation Complex (Fig. 5), which is highly heterogeneous and unpredictable in terms of lithology and permeability; therefore, it may act as a localized aquifer or aquitard (Golder Associates, 2021). Due to this uncertainty, this unit was not mapped as part of a specific aquifer unit. Also, even though the study site is in a high-

latitude region where permafrost might be abundant, the Carmacks area has very limited permafrost (Bonnaventure et al., 2012; Cronmiller et al., 2020).

2.3.2 Modeling Tools

HydroGeoSphere (HGS) is a groundwater modelling program that uses a control volume finite element approach to simultaneously simulate coupled surface and subsurface (saturated/unsaturated) flow and solute transport in three dimensions at each time step (Aquanty Inc., 2015). These features make HGS suitable for this research in which the interactions between surface water (the Yukon River) and the adjacent groundwater aquifers are proposed to be examined under transient conditions. In addition, GRID-BUILDER (McLaren, 2011) was used to generate a 2-D finite element triangular mesh for the selected irregular model boundary, which was subsequently imported into HGS for developing a 3-D triangular prism mesh. Tecplot 360 (Tecplot) was used for visualizing and interpreting model simulation results.

2.3.3 Model Construction

2.3.3.1 Domain Area

Fig. 6 illustrates the boundary of the model domain area. The model boundary follows topographic ridges where it can be assumed to be a divide for groundwater flow and surface runoff and incorporates the majority of the Carmacks community including the drinking water well network. The overall size of the model domain is 31.7 km^2 and it captures a large reach of the Yukon River and a portion of the Nordenskiold River, which flow through the Carmacks area.

2.3.3.2 Discretization

The model domain was first discretized into a 2-D triangular finite-element mesh in GRID-BUILDER. The area within the point bar was refined with an element length of approximately 60 meters to minimize the Peclet number, which can improve the accuracy of solute transport simulation (Daus et al.,1985). In addition, the coordinates of the public supply well, PW-05, were imported into GRID-BUILDER using the “Make wells” function (McLaren, 2011). Elements near PW-05 were further refined automatically, which makes the element length shorter than 10 meters near the refinement center in order to more effectively capture changes in the piezometric surface as a result of

groundwater extraction. Outside these refined areas, the element length was approximately 150 meters on average.

Ground surface elevation (LiDAR) data for the study site (1-meter resolution; Government of Yukon, 2019), available within the same coordinate system as the 2-D mesh, were loaded in HGS and assigned to the 2-D mesh. Because the LiDAR data do not contain elevation information for the streambed, the streambed elevations of the two rivers were manually assigned in QGIS by assuming a 2 to 10 m difference between the river thalweg and the adjacent river bank. The river channels were assumed to have an approximately trapezoidal shape. HGS builds layers in the vertical direction, working downward from the surficial 2-D mesh. The bottom of the model, which represents the top of the Carmacks Aquitard, was assumed flat, with an elevation equal to 475 m. The vertical domain was split into 27 layers using the "proportional sublayering" command in HGS (Aquanty Inc. 2015), which discretizes the model into 20 thin layers near the top and 7 thicker layers near the bottom. The top layer of the mesh is the overland flow domain (OLF), and the 27 layers below it constitute the porous medium domain (PM). The Dual Node scheme was used to couple these two domains together. The entire domain (OLF and PM) involves 136,532 nodes and 258,384 elements. Fig. 7 shows the discretized conceptual model in three dimensions.

In order to solve the flow and transport equations, we choose the finite-difference method instead of the default finite-element method in HGS. Finite-difference method is more suitable for our study which involves overland flow and the unsaturated zone, thus requiring the solution of non-linear equations. The finite-difference method is more robust than the finite-element method when solving non-linear equations and tends to converge more easily (Y. J. Park, personal communication, March 14, 2023). The HGS model is able to use finite-difference formulation to solve flow and transport equations for 2-D triangle and 3-D triangular prism elements (Aquanty Inc, 2015).

2.3.3.3 Field Data and Model Parameters

After the simulation domain was established, field data were collected and analyzed to support the conceptual hydrogeologic model. The (arithmetic) average hydraulic conductivity for the aquifer unit (Łots'an aquifer) near PW-05 was reported as $2.4 \times 10^{-4}\ m/s$ based on pumping test interpretations (Morrison Hershfield, 2020). This falls into the range of hydraulic conductivity values for unconsolidated silty sand and clean sand (Freeze & Cherry, 1979). Due to the absence of hydraulic conductivity measurements at other locations of the study site, the two unconfined aquifers were

assumed to be one continuous, homogeneous unit, which share the same hydraulic conductivity value estimated at PW-05. Although considered homogeneous, the aquifers were assigned a vertical to horizontal anisotropy ratio equal to 0.5, which is within the range of anisotropy ratios for fluvial aquifers (Todd & Mays, 2005). The representativeness of this bulk value of hydraulic conductivity was further explored during the model calibration process.

In summary, the aquifer unit in the numerical model was represented as a homogeneous and anisotropic medium with a saturated hydraulic conductivity (K_{sat}) equal to $2.4 \times 10^{-4}\ m/s$ in the horizontal directions (x and y) and $1.2 \times 10^{-4}\ m/s$ in the vertical direction (z). In addition to the hydraulic conductivity, the aquifer unit was assigned a porosity of 25%, a value within the range for unconsolidated gravel and sand (Freeze & Cherry, 1979). Morrison Hershfield (2020) also used this porosity for PW-05 capture zone delineation. The specific storage used in this model was assigned to be $5.0 \times 10^{-4}\ m^{-1}$, based on literature values for loose sand material (Batu, 1998).

In addition to the aquifer unit, the model also includes bedrock and the McConnell Ice Stagnation Complex units. The bedrock unit was assumed to be isotropic and homogeneous, and based on the primary formation of the bedrock unit as discussed above, which are igneous rock (basalt) and sedimentary rock (sandstone), the bedrock unit was given a hydraulic conductivity of $1.0 \times 10^{-10}\ m/s$ and a porosity of 5% as suggested by Freeze and Cherry (1979). Meanwhile, the McConnell Ice Stagnation Complex unit within the model domain, which was reported to be unpredictable in lithology and hydraulic properties (Golder Associates, 2021), was assumed to act as a localized aquitard and share the same hydraulic parameters as the bedrock unit. Fig. 8 is a plan view map shows the distribution of the bedrock and the McConnell Ice Stagnation Complex units and the aquifer unit in the numerical model.

Fig. 9 shows the locations of all the data collection points used to obtain relevant field data. A gauging station on the Yukon River (09AH001) was used to record the river flow rate from 1951 to 1994 (Water Survey of Canada [WSC], 2023a). The gauging station was not in operation between 1994 and 2014. Since 2014, the station has been used for river stage measurement only. As there are no simultaneously recorded flow rate and river stage data, it is not possible at this time to generate a rating curve to calculate flow rates from recent river stage measurements. Another gauging station located upstream of the model domain and on the Nordenskiold River (09AH004) offers river flow rate measurements since 2011 (WSC, 2023b). In addition to the river stage and flow rate data, the

Meteorological Monitoring Station operated by Environment and Climate Change Canada (ECCC) provides daily precipitation data since the year 1999 (ECCC, 2023). The measured data at this station were assumed to represent the precipitation record within the model domain.

Groundwater level measurements at multiple locations were also collected (Fig. 9), including the well labeled as Carmacks Grader Station with Borehole ID: 980000242, the well labeled as Carmacks Sewage Lagoon - MW02 with Borehole ID: 980000859, and the well labeled as Carmacks SWDF-MW06 with Borehole ID: 980000296. These three wells provide groundwater level measurements near the model domain boundary and detailed information for these wells can be found on theYukon Water Well Registry website (https://yukon.maps.arcgis.com/apps/webappviewer/index.html?id=51322dfb133d42c4ad184fee9986048b). In addition, Core 6 Environment (2020) reported that in 2018 twenty-one monitoring wells were installed in the Village of Carmacks (near the southeast of the riverbank, as the inset map shows) in order to investigate contaminant transport and groundwater flow for environmental site assessment (Fig. 9). Groundwater levels at these monitoring wells were measured several times during 2018 and 2019 and these monitoring wells are referred to as the South Riverbank Groundwater Monitoring Wells in this presented study. Another monitoring well with site code YOWN-2006S measured groundwater levels at the west side of the riverbank (Fig. 9) since 2021. Information on this well can be found on the Yukon Water Data Catalogue website (https://yukon.maps.arcgis.com/apps/webappviewer/index.html?id=2365a4c0b8744f34be7f1451a38493d2). In addition, the pumping rate of the municipal water supply well (PW-05) in the Water Treatment Plant was reported as $2L/s$ (Morrison Hershfield, 2020).

The hydraulic properties selected for the geologic materials within the model – including hydraulic conductivities, storage coefficients, and porosity – were assigned to the conceptual model as domain properties and were not modified as part of the calibration process. Other field data including river flow rates, areal precipitation, groundwater level measurements, and the public well pumping rate were used to assign model boundary conditions and calibrate the numerical model, which will be discussed in the following sections.

2.3.3.4 Boundary Conditions

Fig. 10 illustrates the boundary conditions that are assigned to the surface and sub-surface of the model domain. The locations where the Yukon River and the Nordenskiold River flow into the OLF

domain were assigned nodal volumetric flux $[L^3/T]$ values to represent the inflow of river water. Meanwhile, the Yukon River channel outlet was assigned a critical depth boundary condition that forced the water depth at the outlet equal to the critical depth (Aquanty Inc, 2015), enabling surface water to exit through the channel outlet. The validity and utility of using a critical depth boundary at the river channel outlet or the outer boundary of the OLF domain has been proven by others (Hwang et al., 2014; Schilling et al., 2019). In addition, the surface of the OLF domain (except for the river channels) was given a specific flux $[L/T]$ boundary condition to represent areal rainfall. Net precipitation was assumed to be one-third of the total annual precipitation, which is the sum of the daily precipitation measured in 2021 at the Meteorological Monitoring Station (Fig. 9), after estimated losses from evapotranspiration processes are accounted for. The ratio of evapotranspiration to the total precipitation was adapted from research conducted within the Yukon River Basin by Yuan et al. (2012). The net precipitation was divided by 365 days to calculate the daily net precipitation value which was applied to the model as a specific flux $[mm/day]$ boundary condition.

As Fig. 10 illustrates, within the subsurface domain, a no-flow boundary condition was assigned to the lateral boundaries that follow topographic ridges. However, model boundaries at the west, south, and northwest sides that intersect with floodplain with relatively low surface elevations cannot be treated as groundwater flow divides; therefore, the boundary conditions for these locations became more complex. Where the boundary interacts with the fluvial plain along the east and northwest sides, a no-flow boundary condition was applied to the upper (vadose zone) layers and a constant-head boundary condition was applied to the deeper layer, which is similar to the work by Chow et al. (2016). The water table that separates the vadose zone and the underlying saturated media was estimated based on the groundwater level measurements at the Carmacks Grader Station and the Carmacks Sewage Lagoon - MW02 (Fig. 9). With these special boundary condition settings, groundwater is flowing into the model domain through the east flood plain (upstream direction) and out through the northwest flood plain (downstream direction), which represents the regional groundwater flow within a river-connected aquifer floodplain. Unlike the east and northwest sides, the fluid transfer (third type) boundary condition was applied to the south of the model domain (the South Valley), as Fig. 10 shows, because recorded groundwater levels at the Carmacks SWDF-MW06 (Fig. 9) were available and the groundwater flow direction is unknown. Additionally, a nodal volumetric flux that was reported as $2L/s$ was specified at PW-05 (red dot in Fig. 10) to represent the pumping rate of the public water supply well (Morrison Hershfield, 2020).

2.3.3.5 Model Calibration

The numerical model results were calibrated to observed river stage and groundwater level measurements to ensure that the boundary conditions are reasonably defined and tuned to represent the field situation. As WSC (2023a) reported, the river stages at the Yukon River Gauging Station (09AH001) on August 13, 2019, and October 3, 2019, were 518.9 and 518.6 masl, respectively. Meanwhile, Core 6 Environmental (2020) measured the groundwater levels at the South Riverbank Groundwater Monitoring Wells on August 13, 2019 and October 3, 2019, which were used as calibration targets. Another calibration target was the measured groundwater levels at the YOWN-2006S when the river stage is at 518.9 and 518.6 masl. The model calibration process was performed twice as the following describes.

First, the flow rate of the Yukon and Nordenskiold Rivers, as well as the boundary conditions in the porous media domain, were adjusted manually to ensure that the steady state model results met the following requirements: 1) the simulated river stage at the Yukon River Gauging Station (09AH001) matched well with the observed river level on August 13, 2019, which is 518.9 masl; 2) the simulated groundwater levels at the South Riverbank Groundwater Monitoring Wells matched with the observed levels on August 13, 2019, as much as possible; 3) the simulated groundwater level at the YOWN-2006S matched with the measured level as closely as possible; and 4) no unexpected overland flooding developed.

After the above requirements were met, the flow rate of the Yukon River was updated and the model was run to a steady state, which allowed the simulated river stage at the Yukon River Gauging Station (09AH001) to match with the observed river level on October 3, 2019, which is 518.6 masl. Then the calculated groundwater levels at the South Riverbank Groundwater Monitoring Wells were compared to the measured data on October 3, 2019, to ensure an acceptable fit. The calculated groundwater level at the YOWN-2006S was also compared to the measured level to ensure a good match.

After calibration, the Nordenskiold River inflow rate and boundary conditions in the porous media domain of the model were not changed during the subsequent numerical simulations. That is, the Nordenskiold River inflow rate and the subsurface environments at the model boundaries were assumed independent of the fluctuating river stage of the Yukon River.

2.3.4 Modeling Approach

2.3.4.1 Steady State Well Capture Zone

As discussed previously, backward particle tracking is a common method to generate steady state well capture zones. However, only forward particle tracking is available in HGS. Therefore, the "streamtraces" function of Tecplot, which works similarly to a backward particle tracking algorithm, was used to visualize the capture zone of the pumping well, PW-05. Tecplot calculates the travel path of arbitrarily placed, massless particles under steady state conditions, based on the user-defined vector field (Tecplot Inc, 2022). In the present study, the groundwater velocities in the x, y, and z directions are computed by HGS at each node within the simulation domain and are the components of the vector Tecplot uses for travel path mapping. Once the massless particles are placed, the direction in which the streamtraces are drawn can be selected as "backward", which means the particles will be traced backward from their starting position, following the velocity vector fields. The starting position can be one individual point or a group of points that are evenly distributed along a selected distance. In our study, a group of massless particles were placed very close to the well screen of PW-05 and traced in the backward direction to visualize the steady state well capture zone.

2.3.4.2 Transient Well Capture Zones

In addition to the steady state case, this research also sought to analyze the well capture zones under fluctuating river stages that lead to transient groundwater flow conditions. The streamtraces function of Tecplot was again used for delineating the well capture zones. In contrast to the steady state simulations where the flow field remains constant in time, the transient simulations produce a constantly changing groundwater flow field. In order to investigate how the well capture zone would change as the river stage rises and falls, a series of output times were specified during the river stage fluctuation period and the velocity field provided by the model at each point in time was used by Tecplot to produce stream traces and related capture zones. As a result, a series of different capture zones were delineated as an indication of how the changing river stage influenced where groundwater was being captured by the pumping well.

2.3.4.3 Advective Travel Time Analyses for Steady State

Another feature of the streamtraces function in Tecplot is estimating the travel time along the complete streamtrace. In order to complete this, a time interval is assigned so that Tecplot can draw

stream markers along the streamtraces where the distance between each marker equals the product of the time interval and the local groundwater vector fields (Tecplot, 2022). Because we want to know the travel time of numerical particles travelling from the streambed (Yukon River) to the well screen within the aquifer, the streamtraces that original at the streambed and arrive at the well were selected for drawing stream markers.

According to the method in which stream markers are drawn, the travel time only accounts for the advection process and is dependent on the velocity vector fields provided by the model within the simulation domain. For a model in steady state condition, the stream markers on each streamtrace reflects the advective travel time for a particle travelling from the starting (well screen) to the ending position (streambed) along that streamtrace. The travel time was estimated at each streamtrace, and the shortest travel time was identified for further comparison within different simulation scenarios.

2.3.4.4 Well Vulnerability Assessment

One drawback in the discussed methods for capture zone delineation and advection travel time estimation is that dispersion, which is an important mechanism in solute transport, is ignored. To account for the dispersion mechanism to evaluate the vulnerability of the water supply wells (public and private) in Carmacks under the influence of variation in the Yukon River stage with more accuracy, forward solute transport was employed.

Solute with a fixed concentration equal to 1.0 (units arbitrarily kg) was constantly injected into the model domain through the inflow nodes of Yukon River at the model boundary. Here the solute is conservative and non-reactive and represents possible contaminants carried by the Yukon River. The solute tracer was configured to appear in the river at the start of the simulation and be constantly injected into the surface water until the simulation concluded. This represents the worst-case scenario in which the water wells may become unsafe to use as the result of annual floods.

In order to examine the influence of river stage variations, forward solute transport was run under four different scenarios that will be explained later. All four scenarios were run for 10 years into the future, which is a time that is long enough for the solute plume to migrate to the water wells and attain a relative solute concentration that is detectable and sufficient for the desired analyses. The simulation time could be extended for decades, but this was unnecessary to fulfill the objectives of the present study.

A relative concentration of 10^{-4} was chosen, following Frind et al. (2006), as a threshold to determine when the contaminants should be considered to be "arriving" and compromising the water quality of the wells. The time taken to breach this threshold was used for well vulnerability analysis by comparing it to at travel time of 50 days, which is often used for identifying GUDI wells as mentioned in the Background section.

2.3.4.5 Basement Foundation Inundation Analysis

The risk and duration of the basement inundation for buildings located near the Yukon River in Carmacks were evaluated by comparing the simulated water table to the estimated basement elevation at chosen observation points (Fig. 11). Each observation point was placed below the steady state water table and will remain fully saturated during flood events, representing the local water table position. The basement elevation at each observation point was assumed to be three meters below ground surface elevation; therefore, the estimated basement elevations are not all at the same level. For each observation point, basement inundation was assumed to occur when the simulated water table rises to or above the estimated basement elevation, and the issue ends once the water table drops below the estimated building basement.

2.3.4.6 Simulation Scenarios

The objectives of the numerical experiments were to quantify the influence of the annual variation in the Yukon River stage on the water quality vulnerability of drinking water wells in Carmacks and on the occurrence of inundation of household basements for homes located adjacent the river. In order to examine these processes, two steady state and two transient modeling scenarios were developed.

The first steady state scenario was designed to represent conditions immediately prior to the start of the increase in river stage due to the spring freshet. This scenario utilizes an average river stage over an annual cycle. This will be referred to as the base case scenario. This scenario also represents the initial conditions prior to the transient increase and decrease in Yukon River stage associated with the spring melt period.

The second steady state scenario was assigned a higher Yukon River flow rate than that in the base case scenario, which makes the simulated, steady state river stage peak close to the highest recorded level in 2022. This scenario will be referred to as the steady high-level scenario. This is a very simple scenario designed to evaluate the influence of higher river stage on well vulnerability and basement

inundation. The model results derived from this scenario will be compared to the results from the transient scenarios, which are described below, to examine the differences in well vulnerability assessment between using an easy-to-setup steady state model and a more realistic, yet more complicated transient model.

As discussed earlier, the highest annual level of the Yukon River stage has been observed to be increasing in recent years as compared to the past, based on available data. In order to examine the potential impact of these annual higher river stages on well vulnerability and foundation inundation with a more realistic model, two transient scenarios were designed. The first transient scenario employs the average annual transient river stage based on historical data. This is intended to represent typical conditions within the Carmacks region and can be used to quantify well vulnerability and inundation potential under average annual conditions. This will be referred to as the typical annual variation scenario. The second transient scenario utilizes higher spring river stages, as have been recorded in recent years, to examine any potential enhancement in drinking well vulnerability and basement inundation as a result of the higher river stage. This will be referred to as the extreme annual variation scenario. The typical annual variation scenario includes the simulated river stage peaks between the 10-year and 50-year return period levels of the Yukon River at Carmacks (Government of Yukon, 2022a). In contrast, the extreme annual variation scenario has simulated river stage peaks above the 200-year return period level (Government of Yukon, 2022a).

The transient simulations start with the steady initial condition derived from the base case scenario, and the river stage is progressively increased and reduced in accordance with the recorded river level data for the two scenarios over an entire annual cycle. The simulations are extended over several years for both transient scenarios, and river stage continuous to fluctuate in an annual basis during the extended simulations. Using the streamtracing methods, forward solute transport simulations, and water table elevation comparisons as outline above, insight into the influence of the transient Yukon River stage on the public and private drinking water wells, along with the foundation inundation potential, are examined in detail.

2.4 Results and Discussions

2.4.1 Calibration Results

In order to demonstrate that the model is providing a reasonable representation of the physical conditions at the study site, an initial steady state simulation was compared to a series of twenty-six calibration points, which are points where groundwater levels have been measured in the past. The locations of these calibration points are shown on Fig. 9. Fig. 12 demonstrates the numerical model calibration results. The observed data on August 13, 2019, and October 3, 2019, are compared with the simulated head values as discussed in the Methodology section. The calibration plots show that the simulated head values match the observed data with a reasonable fit ($< 40\ cm$ in all cases). The average absolute errors for the calibration results on August 13, 2019, and October 3, 2019, are 8.2cm and 12.9cm, respectively. However, four calibration targets are labelled on the plots, where the simulated head values deviate from the observed values with a larger absolute error. As the plot indicates, the calibration targets MW-1 and MW19-13 have a simulated head value approximately 30cm smaller than the observed head value in both calibration cases. In addition, the MW19-14 and the YOWN2006-S have simulated heads 13cm and 17cm smaller than the observed head values in the calibration case of October 3, 2019.

The locations of the four calibration targets where agreement with the simulation results is relatively poor can be found in Fig. 9 (MW-1, MW19-13, MW19-14 and YOWN2006-S). A possible reason for the deviations between the simulated and the observed head values is potential local, small-scale heterogeneity, which is not included in the numerical model. Another possible reason is that the river-connected aquifer at the study site is always in the transient condition due to river level fluctuations. Thus, the collected head values during the two days and the corresponding measured groundwater level at YOWN2006-S are associated with a changing environment. These collected data were used to calibrate the numerical model, which runs to a steady state, and could cause the deviations as observed from the plots. However, considering that most calibration targets have an acceptable fit between the observed and the simulated head values, these poorly matched locations are anticipated to have negligible influences on model simulation results.

2.4.2 Simulated Hydraulic Head Under the Base Case Scenario

Fig. 13 demonstrates a horizontally placed slice in the saturated porous media domain showing the calculated hydraulic heads under the base case scenario, where the red dashed lines indicate the overall regional groundwater flow directions. Fig. 13 shows that most of the model boundary has groundwater flowing into the model, except for the northwest and the southwest of the model domain, where groundwater flows out of the model. In addition, the impact of pumping groundwater from the water treatment plant in the center of the point bar, which is an alteration of local groundwater flow direction, is visualized by calculated hydraulic head and groundwater flow lines.

2.4.3 Simulated River Stage Under the Transient Scenarios

Fig. 14 shows the simulated annual river stage variation cycle in the typical and extreme annual variation scenarios. As discussed previously, the annual river stage variation cycle in both transient scenarios starts with the steady initial condition derived from the base case scenario; therefore, it can be noticed from the plot that the simulated river stage is a constant value prior to the river stage variation period. During the river stage variation period, as indicated in the plot, the simulated river stage starts to progressively rise from the low level (river stage rising period) and peaks in accordance with the historical trend, following a progressive decline (river stage recession period) before the simulated river stage decreases to the pre-variation level. After the river stage variation period, the simulated river stage will again maintain a level that equals the pre-variation level during the remaining annual river stage cycle.

Although the simulated river stage in the two scenarios has the same increasing and decreasing trends, the simulated river stage peaks at a higher level in the extreme annual variation scenario (Fig. 14b) than in the typical annual variation scenario (Fig. 14a). Again, this is intended to represent and accommodate the extreme annual variation scenario recently observed where the river stage peaks at a higher level during the spring melt period than is normally observed. Each transient scenario will repeat the corresponding simulated annual river stage cycle throughout the entire simulation.

2.4.4 Streamtracing Results of the Municipal Pumping Well (PW-05)

Fig. 15 shows the streamtracing results of the base case scenario. Most streamtraces are oriented from southeast (SE) to northwest (NW) and extend in the SE direction. Streamtraces are confined within the point bar, with some travel paths touching the edge of the river channel but not crossing beyond it.

In addition, some streamtraces also originated from the ground surface, as the cross-section diagram shows. The streamtracing results represent the steady state well capture zone, which illustrates that PW-05 draws water from the aquifer recharged by surface infiltration and from the adjacent Yukon River when the river stage is maintained at the average annual level.

Fig. 16 and Fig. 17 illustrate the streamtracing results at six output times during an annual river stage cycle of the typical and extreme annual variation scenarios, respectively. Among these six output times, 151 days and 178 days are two model output times that correspond to the river stage rising period of the annual cycle, whereas 190 days and 262 days correspond to the river stage recession period. The other two model output times, 70 days and 365 days, correspond to times before and after the river stage variation period.

As mentioned, the two transient scenarios utilize the model results from the base case scenario as the initial conditions. Therefore, the streamtracing results before the beginning of the annual river stage variation (Figs. 16a and 17a) are identical to the base case scenario streamtracing result (Fig. 15). However, it is clearly illustrated by Figs. 16b, 16c, 17b, and 17c that, compare to the streamtracing results for the base case scenario (Fig. 15), the streamtraces during the river stage rising period become more concentrated with their overall orientation shifting to a SW-NE direction. While Figs. 16b and 16c demonstrate that the streambed of the Yukon River can be the origin of the streamtraces during the river stage rising period of the typical annual variation scenario, Fig. 17c shows that the edge of the point bar can temporarily become the origin of the majority of the streamtraces. The overland flood area near the edge of the point bar simulated by the numerical model in the extreme annual variation scenario could be the reason for this streamtrace pattern. These streamtracing results also indicate that the rising river stage could temporarily change the groundwater flow direction within the point bar and therefore alter the size and orientation of the well capture zone as well as the primary water source for the well. The altered groundwater flow direction and well capture zone under the rising river stage may also change the travel time for river water to be captured by the pumping well, which will be examined later.

On the other hand, Figs. 16d, 16e, 17d, and 17e demonstrate the streamtracing results during the river stage recession period of the two transient scenarios. Under both scenarios, the streamtraces become less concentrated, and their overall orientation shifts back to SE-NW as the river stage decreases. In addition, the ground surface again becomes an origin of some of the streamtraces. These

results indicate that the aquifer underneath the point bar, which has been replenished by the river during the previous river stage rising period, again contributes water to the pumping well during the river stage recession period. Figs. 16f and 17f show the streamtracing results three months after the river stage decreased to the pre-variation level. The streamtracing results in the top and cross-section views are very similar to the results at 70 days, which might indicate that the flow fields have mostly recovered to the pre-variation conditions.

It should be reiterated that the streamtraces are drawn solely based on the groundwater velocity fields without the ability to quantitatively reflect the contribution area of yielded water at PW-05 under transient conditions. However, the streamtracing results illustrate the intense shifting in the size and orientation of the area that may contribute water to the pumping well, as well as the possible temporary change of water sources during the fluctuation of the river stage.

2.4.5 Stream Markers Results of the Municipal Pumping Well (PW-05)

Fig. 18 illustrates the stream markers resulting under the base case and steady high-level scenarios. The stream markers, which are yellow spherical dots in each scenario, are distributed along streamtraces that are connected to the streambed and the well screen. The time interval between each yellow dot is ten years. The count of stream markers on each streamtrace indicates the time a particle requires to travel from the starting point (streambed) to the well screen along a streamtrace. As can be observed in Fig. 18, streamtraces contain more stream markers in the base case scenario than in the steady high-level scenario. The estimated shortest travel time in the base case scenario, as indicated by the streamtrace with the least number of yellow dots, is 40 years. In contrast, the estimated shortest travel time in the steady high-level scenario is 20 years. The difference in the shortest advective travel time from these two steady state scenarios indicates that a higher river stage may accelerate groundwater flow from the river to the well screen resulting in shorter travel times.

2.4.6 Forward Solute Transport Simulation Results and Breakthrough Curves of the Municipal Pumping Well (PW-05)

Fig. 19 demonstrates the relative concentration of a river-origin solute captured by PW-05 under the four scenarios. A log scale is used on the y-axis for plotting the relative concentration so the threshold level and the breakthrough curves in different scenarios are easy to compare. A minimum relative concentration level of 10^{-6} was selected as the origin point of the y-axis. A horizontal dashed line

that corresponds with the relative contaminant concentration threshold value is drawn to examine the time to breach this level under different scenarios.

As seen in Fig. 19, breaching the threshold in the base case scenario takes longer than six years. This breach time means that it would take the river-origin solute more than six years to reach the critical relative concentration threshold at the pumping well if the Yukon River maintains its average level and does not fluctuate annually. However, the breaching time is less than two years if the Yukon River maintains the highest level, according to the breakthrough curve of the steady high-level scenario. The shorter breaching time in the steady high-level scenario indicates that the solute migrates faster towards the pumping well when the river level is higher, which aligns with the results from the advective travel time analysis discussed above. However, the breaching times obtained from the breakthrough curves for the two steady scenarios are much shorter than that estimated from the stream markers. One reason for this is that the forward solute transport simulations consider the dispersion and the advection processes. In contrast, the advection process is the only factor determining the advective travel time. Another reason is that a relative concentration threshold level was applied instead of using virtual particles to determine the “arrival time”.

Fig. 19 also presents the time to breach the threshold level under the two transient scenarios. As the plot shows, it takes about 4 years (typical annual variation scenario) or 2.5 years (extreme annual variation scenario) to breach the threshold level. Compared to the breaching time in the base case scenario, the annual river stage variation can accelerate the solute transport from the source (river) to the receptor. The acceleration is positively related to the magnitude of the river stage variation.

Another observation that can be derived from the results in Fig. 19 is that the breaching time obtained from the extreme annual variation scenario is longer than that from the steady high-level scenario; however, the steady river stage in the steady high-level scenario equals the peak river stage during the annual river stage cycle in the extreme annual variation scenario. This illustrates the importance of employing transient model scenarios rather than a simple steady state model while evaluating the well vulnerability. As the plot shows, the breakthrough curve of the steady state scenarios is smooth whereas the breakthrough curves of the transient scenarios have pulses. The pulses on the breakthrough curves indicate the progression and recession of the solutes in the point bar under the influence of rising or declining river stages. The pulses on the curves match with the theory of groundwater-surface water interactions under fluctuating river stages, which is explained by

Winter et al. (1998). Appling their theory in this case study, solute in the Yukon River will be carried into the point bar through a process termed “bank storage” during the river stage rising period; however, the solute will be partially flushed out during the river stage recession period when the water table is higher than the river stage, and groundwater within the point bar starts draining back to the Yukon River. These special processes are associated with river stage variation and cannot be reproduced by a simple steady state scenario with a fixed, higher-than-average river stage.

In a summary, even though under the extreme annual variation scenario, river-contained contaminants are shown to breach the limited threshold level after 2.5 years, the breaching time is still much longer than 50 days which is used to identify a GUDI well. Therefore, the model indicates that even if the extreme river stage variation occurs annually, the PW-05 is likely to be protected from microbial pathogens that may be present in the Yukon River.

2.4.7 Basement Inundation Analysis for Observation Points at South Riverbank

Fig. 20 and Fig. 21 illustrate the simulated river stages at the river gauging station and water table elevations at observation points S1, S3, S5, and S7 (Fig. 11) during the river stage cycle of the typical annual variation scenario and the extreme annual variation scenario, respectively, with estimated basement elevation added for evaluating basement inundation. The plots exclude simulation results prior to the river stage variation period (the first 147 days), and, therefore, only show the results of the last 218 days.

Fig. 20 and Fig. 21 show the estimated basement elevation at each observation point as a fixed value. The water table elevation and river stages are constantly changing due to the fluctuating river stage in the Yukon River. In both scenarios, the water table rises from its steady state position immediately as the river stage begins to increase and peaks after about 30 days since the beginning of the river stage variation, then slowly returns to the pre-variation level during the river stage recession period.

The estimated house basement elevation was compared with the fluctuating water table. In Fig. 20, the simulated water table at S1, S3, and S7 does not rise above the estimated house basement, which means the river stage variation in the typical annual variation scenario would be less likely to cause basement inundation for buildings at these locations. However, Fig. 20c shows that the simulated water table overtops the estimated basement at S5 and causes basement inundation that lasts about 25 days, which indicates house basements near S5 might be impacted by the fluctuating river stages.

On the other hand, Fig. 21 shows that the river stage variation in the extreme annual variation scenario might cause basement inundation issues for more households at the south riverbank. As Figs. 21a, 21c, and 21d indicate, the water table will overtop the estimated basement at S1, S5, and S7 after about 20 days since the river stage starts rising. However, the duration of the basement inundation at these three locations is different. While the basement inundation issue lasts about 40 days at S5, houses at S1 and S7 are impacted by the elevated water table for 30 days and 20 days, respectively.

Although the annual river stage variation may impact the basements at S1, S5, and S7, households at S3 will likely remain free of influence as Figs. 20b and 21b indicate. There are two possible explanations why the river stage variation would have less of an impact relative to basement inundation at the S3 location. First, the greater ground surface elevation at S3 makes the estimated basement about 1m higher than S1 and S7 and 1.5m higher than the basement elevation at S5, which might explain why the elevated river stage does not impact the basement at S3. The relatively low elevation of the estimated basement at S5 also explains the basement inundation issue at S5 during the typical river stage variation. Another aspect is that the water table at S3 is less sensitive to the river stage variation. That is, the rise of the water table from the steady state level to the peak level at S3 is less than that at S1 and S7. During the extreme river stage variation event, the water table at S3, which has a pre-variation level of 519.33 masl, rises 1.94m to reach the peak level, whereas the water table rises 2.34m and 2.07m at S1 and S7, respectively.

In addition to risk and duration, the simulated river stage associated with simulated basement inundation at the observation points could be used as a threshold during summer seasons to warn residents living near the riverbank to prepare for possible basement inundation. For example, Figs. 21a, 21c and 21d indicate that the simulated river stage at the gauging station is about 521 masl when basement inundation occurs at S1, S5, and S7. Precautions may be necessary when the monitored river stage at the gauging station approaches this threshold.

2.4.8 Forward Solute Transport Simulation Results and Breakthrough Curves of the Observation Points at South Riverbank

Fig. 22 shows the breakthrough curves at observation point S1, S3, S5, and S7 under the base case scenario, typical annual variation scenario, and extreme annual variation scenario. Again, the solute is constantly injected into the Yukon River from the beginning of the simulations under each scenario. As can be seen, each plot only includes the model results of the first 512 days, which is one whole

annual river stage cycle (365 days) plus time before the next river stage variation period in the following annual cycle (147 days). Instead of using a log scale on the vertical axis to plot relative concentration, a linear scale is used on the vertical axis to plot a zero relative concentration.

As Figs. 22a and 22c illustrate, the relative concentration at S1 and S5 under the base case scenario is zero, which means solutes in the river will be less likely to infiltrate into the riverbank around these observation points when the river level is maintained at the average level. Similarly, the relative concentration at S3 under the base case scenario is not zero but at a very low level (Fig. 22b). However, under the typical and extreme annual variation scenarios, the relative concentration at S1, S3, and S5 all start to increase when the river stage starts to increase during the river stage variation period. The relative concentration at these three observation points peaks before decreasing to a non-zero value.

The solute breakthrough curve near observation point S7 is considerably different from that at S1, S3, and S5. As shown in Fig. 22d, the relative concentration continually increases during the first 512 days under each scenario. River stage variation results in increased relative concentrations compared to the base case scenario. The river stage variation in the extreme annual variation scenario leads to higher relative concentrations than in the typical annual variation scenario (by an order of magnitude at S1, S3, and S5).

The different behaviour of solute transport at different locations along the riverbank is believed to be induced by the dynamics of interactions between the river and its adjacent riverbank. That is, the hydraulic gradient near S7 is always directed from the river toward the riverbank, allowing solutes to be constantly transported from the river to the riverbank through advection and dispersion processes. Therefore, the relative concentration is always increasing during the simulation. Other than at S7, where the direction of the hydraulic gradient is consistent, the rise in river stage during the river stage variation period changes the direction of the hydraulic gradient at S1, S3 and S5. Before the river stage increase, the hydraulic gradients at S1, S3, and S5 are directed from the bank toward the river, which is unlikely to allow river solutes to migrate into the riverbank. But the direction of the hydraulic gradient at these points reverses during river stage rising period, which enables the transport of solutes into the riverbank with increased relative concentration. However, the reversed groundwater flow direction will return to its previous state during the river stage recession period when the water table in the riverbank is higher than the river stage, until the next river stage variation

period. Solute contained in the riverbank will be partially flushed out, which is why the breakthrough curves for the flood scenarios decrease to lower but non-zero values as Figs. 22a, 22b, and 22c indicate.

Regarding well vulnerability, the model results indicate that domestic wells along the riverbank may be vulnerable to contaminants in the river, considering the recurring extreme river stage variations at Carmacks during 2021 and 2022, as discussed previously. In the south-southeast portion of the riverbank, interactions between the Yukon River and the riverbank are sensitive to changes in the river stage. When the river stage of the Yukon River is rising, contaminants within the river water can be migrate into the aquifer within a short period. The threshold relative concentration, 10^{-4}, was again used here to determine the "arrival time" of the river-origin solute at the four observation points. Fig. 22 demonstrates the overall trends of the breakthrough curve; therefore, a low threshold level is hard to be plotted and distinguish from the horizontal axis and Fig. 23 was made to examine the "arrival time." Figs. 23a and 23c demonstrated that the relative concentration at S1 and S5 breach the threshold level less than one day since the river stage variation started (day 147) under both transient scenarios. Fig. 23b shows that for observation point S3, the relative concentration will breach the threshold less than ten days since the river stage variation started. At the southwest portion of the riverbank where the observation point S7 is located, the aquifer is directly replenished by the Yukon River and contaminants in the river can quickly migrate to the aquifer and may be captured by domestic wells, with or without river stage variation. Instead of starting from 147 days, the horizontal axis in Fig. 23d starts from 0 days, which is the moment when solute was injected into the Yukon River. Fig. 23d shows that while the river stage is maintained at the average level, the river-origin solute should be considered "arriving" at the observation point S7 six days after injection. The "arrival times" described above are shorter than 50 days, which means the domestic wells in the south riverbank are likely under the GUDI condition and vulnerable to contaminants in the river.

2.4.9 Visualization of Solute Migration in the Point Bar and the Riverbank

Fig. 24 indicates the location of two cross-sections through the Yukon River that will be used for illustrative purposes. The B-B' cross-section intersects the observation point S1, and the C-C' cross-section intersects PW-05. Along each cross-section diagram, numerical particles were released from within the Yukon River riverbed to examine the interactions between the river and the adjacent aquifer in the high-level flood scenario. The 2-D cross-section slices are transparent so that particle

paths which flow behind the slice are still visible but shown with a faded grey colour. Each subplot includes an inset graph in the up-right corner showing the current river stage (a red dot) along the annual river stage cycle, which is helpful to understand what position the river stage is when drawing the cross-section diagrams.

Fig. 25 shows the water table positions, groundwater flow direction, and solute distribution during the first year of solute transport simulation under the extreme annual variation scenario along the B-B' cross-section. The information presented in Fig. 25a represents the model results before the start of the river stage variation period, indicating that the riverbed of the Yukon River is receiving groundwater from the southern riverbank but also losing water to the point bar (i.e., a flow-through situation). Although the particle path indicates a groundwater flow direction toward the river on the south bank, the river solute has already entered the riverbank, which might be the result of dispersion and lateral solute transport from the surrounding areas. Figs. 25b and 25c, which are associated with the river stage rising period, indicate that the riverbed on the south side, which previously showed groundwater discharge conditions is now experiencing groundwater recharge due to the elevated river stage. The reversal of the water flow direction, as can be seen from the figures, accelerates the spread of the solute plume into the riverbank. However, Figs. 25d, 25e, and 25f, which are associated with the river stage recession period, demonstrate that the reversed flow directions between the riverbanks and the river will return to their initial directions when the river stage starts to recede to the pre-variation level. Therefore, the solute plume stops spreading into the riverbank on the south side and is slowly being flushed out. Compared to the south riverbank, the groundwater flow direction between the river and the point bar reverses only during the river stage recession period, as can be seen from Figs. 25d and 25e, which indicates a more rapid decline of river stages of the Yukon River than the water table within the point bar.

Fig. 26 illustrates the extreme annual variation scenario model results along the C-C' cross-section that goes through PW-05 and a south-west portion of the riverbank. As the particle paths and the solute concentration contours indicate, the riverbank near observation point S7 is always receiving river water during the simulation, and the solute plume continually spreads into the riverbank without being flushed out. The point bar receives water from the river for most of the time but also loses water to the river during the river stage recession period as Figs. 26d and 26e indicate.

2.4.10 Solute Migration Through the Porous Media Model Domain

Fig. 27 shows the distribution of river-originating solute on a horizontal 2-D slice placed in the porous media domain at the same depth as the PW-05 pumping node after ten years of forward solute transport simulation under three scenarios. Each diagram demonstrates the simulation results for the entire slice with an inset that shows the results around the key research area—the point bar and the southern riverbank. The river channel of the Yukon River is indicated with black dashed lines. The previous discussion regarding the dynamics of groundwater-surface water interactions and the influence of annual river stage cycle on solute transportation will again be reviewed but from a top-view perspective, as follows.

As Fig. 27 showed, the overall distribution of solute in the porous media follows the river channel orientation, with the solute plume deviating from the above channel location and covering a larger area. The build-up of solute at the southwest riverbank in all scenarios aligns with the interpretation that groundwater in this portion of the riverbank is continually replenished by the Yukon River. Since the model boundary has fluid transfer as the boundary condition where the solute plume is built-up, the solute near the southwest riverbank will be flushed out of the model domain through the model boundary by groundwater. A wider spread of solute toward the south direction near the south riverbank can be seen in the typical (Fig. 27b) and extreme (Fig. 27c) annual variation scenarios, which might be caused by the overland flood or accelerated solute transport due to the elevated river stage. The simulation results of the typical and extreme annual variation scenarios also show a more obvious propagation of river solute towards the PW-05 and the southeast portion of the riverbank compared to the base case scenario model result. The propagation of solute into the adjacent aquifer in the extreme annual variation scenario is more pronounced than in the typical annual variation scenario.

2.4.11 Exchange Flux Between the Surface and Sub-surface Domain

Fig. 28 shows the exchange flux between the surface domain and sub-surface domain under the base case scenario (Fig. 28a), typical annual variation scenario (Fig. 28b), and extreme annual variation scenario (Fig. 28c). The positive exchange flux numbers represent groundwater discharge to the ground surface or streambed; whereas the negative exchange flux values mean that there is surface water infiltrating and recharging to groundwater. For example, most of the area is covered by the light blue colour (negative value), representing the infiltration of precipitation from surface to sub-surface.

Fig. 28a shows that under the base case scenario, some stream reaches of the Yukon River are gaining stream with positive exchange flux numbers. On the other hand, Figs. 28b and 28c show that most of the stream reaches which were gaining streams in the base case scenario change to losing conditions with negative flux numbers when the river stage rises to a higher stage under transient scenarios. The dynamic interactions between the surface water and groundwater are again visualized here according to the altered exchange flux patterns.

2.5 Conclusion

Four key findings can be concluded from the presented study. First, the streamtracing results demonstrate that the variation in the river stage could temporarily change the groundwater flow direction within the point bar and therefore induce shifting in orientation and extent of the area that contributes groundwater to the pumping well. Thus, areas outside the steady state well capture zone may temporarily become part of the well capture zone under the influence of fluctuating river stages. The temporary contribution area may contain contaminants that could be carried by the dynamic groundwater flow and eventually captured by the pumping well. Therefore, river stage variation can increase the vulnerability of a water supply well that is hydraulically connected to it.

Second, the advective travel time analyses indicate that a steady state model with a higher river stage leads to a shorter travel time for river-origin particles travelling to the well screen, compared to a steady state model with a lower river stage. Meanwhile, model results from the forward transient solute transport simulations show that annual river stage variation can accelerate the migration of river-originating solutes to the well screen. The acceleration is positively related to the magnitude of the river stage variation, and the vulnerability of water wells increases with the accelerated solute migration.

Although the streamtracing and the forward transient solute transport approaches suggest similar results, it was noted that the later approach accounts for the dispersion process and indicates the "arrival time" of a solute according to a pre-defined threshold level, which are advantages over the advective travel time analysis approach. The results also showed the necessity of employing transient model scenarios incorporating changes of river stage instead of relying on a simple steady state model when evaluating well vulnerability. In the case study, a model with a transient scenario was able to reproduce the dynamics of groundwater-surface water interactions under fluctuating river stages, which include the "bank storage" process and the "flush-out" process. However, a steady state

scenario omits the “flush-out” process and indicates a biased solute migration simulation result, which can mislead the well vulnerability assessment.

Results from the forward solute transport simulations illustrate that even though the solute migration is accelerated under the extreme annual variation scenario, it still takes more than 50 days for a conservative river-originated solute to breach the threshold level and be considered to have “arrived” at the well screen of the municipal water supply well, which means the water supply well is not under GUDI conditions and is unlikely to be polluted by microbial pathogens. However, private wells along the riverbank were identified as GUDI wells based on the breach time over the threshold level, which indicates these private wells are more vulnerable to river-originated contaminants compared to the municipal water supply well located in the center of the point bar. The threshold level could be adjusted according to the contaminant species in the Yukon River and the concentration limit at which the contaminant would be considered harmful to human health.

A third key finding is that the numerical model demonstrates that the river stage fluctuations can temporarily alter the regional groundwater-surface water interactions, such as changing a gaining stream reach into a losing stream by reversing the groundwater flow direction. The alteration is regional, which means different locations along the riverbank would react differently to the river stage fluctuation. In the case study, the switching of groundwater-surface water interaction occurs at certain stream reach during the river stage rising period, which facilitates the spreading of river-origin solute into the riverbank. During the river stage recession period, the hydraulic gradient near that stream reach reverses again, allowing water in the riverbank to flow back to the river. However, the switching of groundwater-surface water interaction is absent at the other end of the river meander where the stream reach is consistently a losing stream reach during the river stage rising and recession periods. Therefore, continuously monitoring river stages and water table elevations at different locations along the riverbank may help to identify the interactions between the river and the adjacent aquifer. Shallow wells constructed near ($< 70m$) the riverbank may have high vulnerability and be impacted by river-origin contaminants.

Finally, the model results demonstrate that at the study site, where basement inundation is known to be an issue, the magnitude of the river stage variation could be a controlling factor for the occurrence. The river stage variation in the extreme annual variation scenario was estimated to cause basement inundation problems for more households along the south riverbank compared to the typical

annual variation scenario. In addition, the elevation of the household basement may also play an important role. In our case study, the elevated water table did not impact the basements with the highest elevations. It is also evident that for house basements which are impacted, the duration of the inundation varies with location; however, the inundation occurs essentially simultaneously at all affected basements when the river stage at the gauging station reaches a certain level.

The present study demonstrated the process of using a fully integrated numerical model to evaluate the influence of annual river stage variation on well vulnerability and basement inundation. The findings may be helpful for other communities in cold environments where people rely on groundwater resources situated near a river course and where groundwater vulnerability concerns exist related to seasonally fluctuating river stage.

2.6 Figures

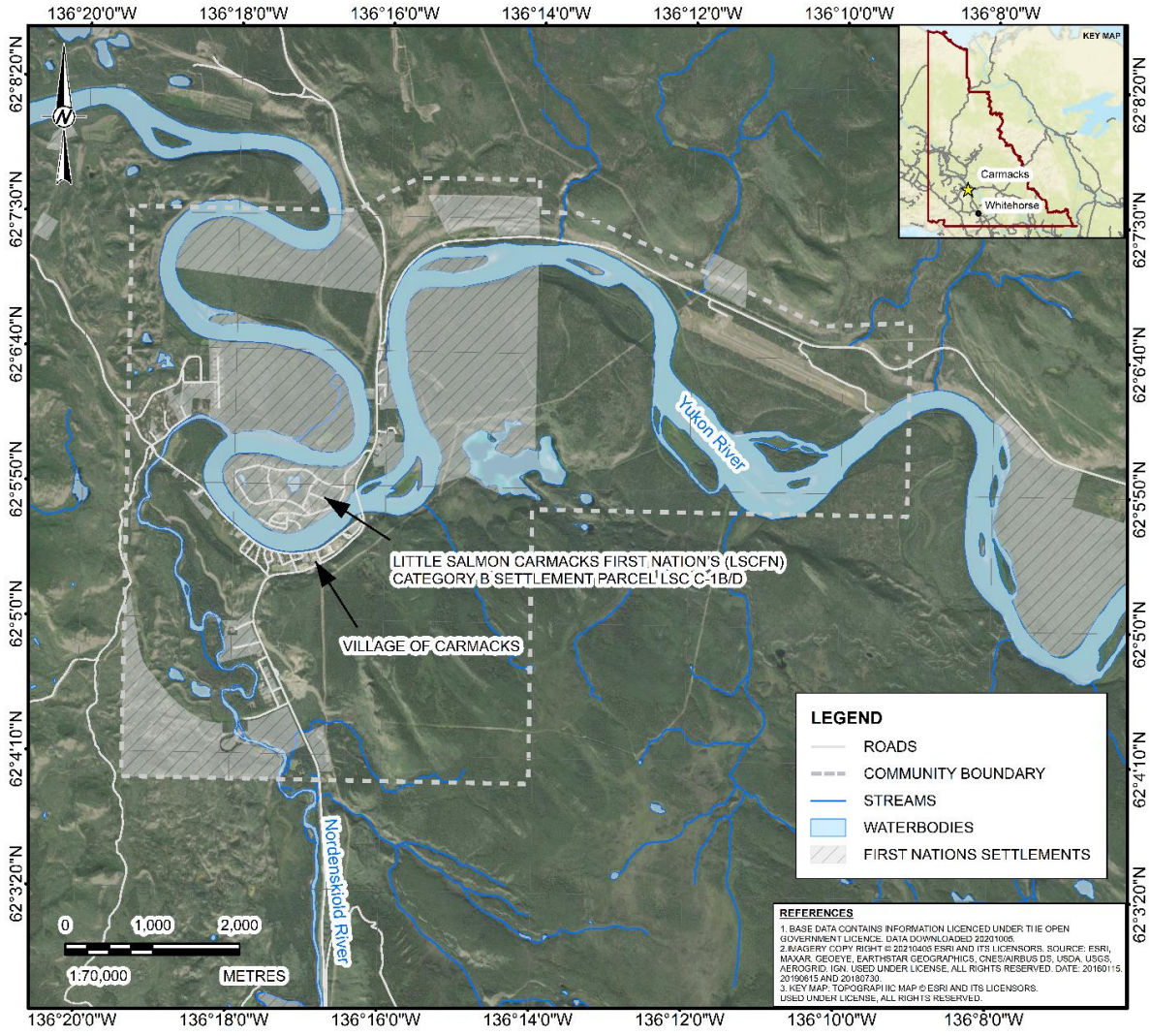

Figure 1. Regional location map of the community of Carmacks (the study site). (Source: adapted from Golder Associates, 2021)

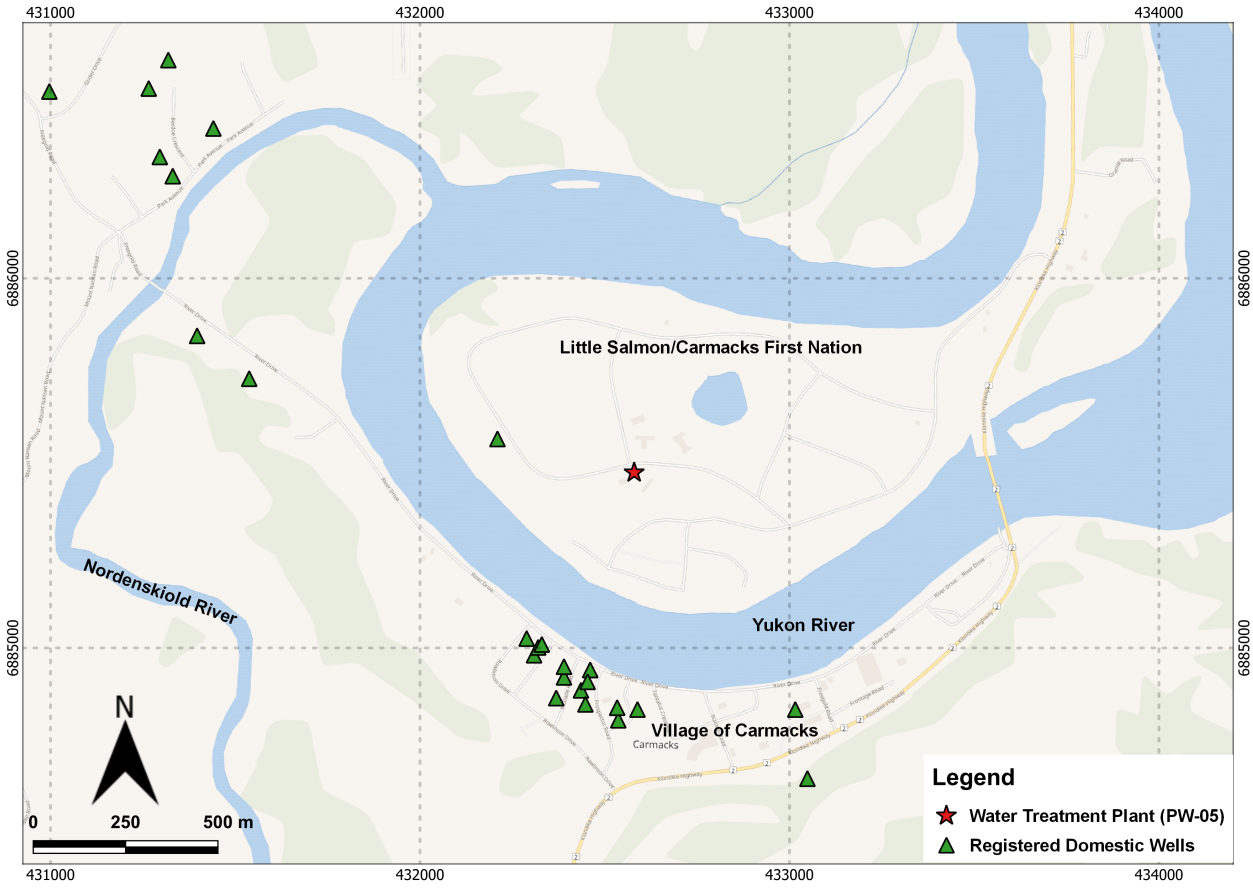

Figure 2. Location of the water treatment plant (PW-05) and the registered domestic wells within the community of Carmacks. Well locations data are from Government of Yukon (n.d.). Background map data: © OpenStreetMap (2023).

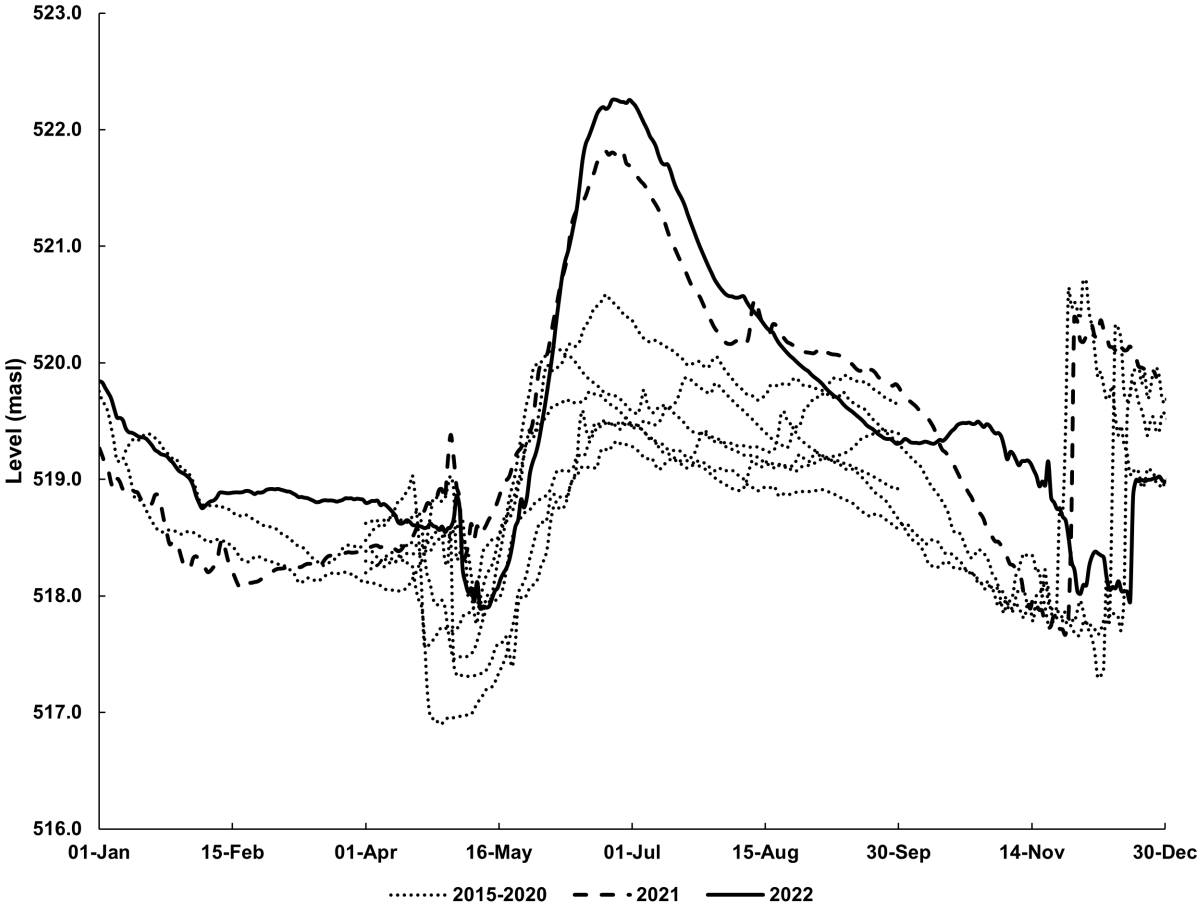

Figure 3. Observed river stages of the Yukon River between 2015 and 2022, data retrieved from a gauging station (09AH001) in the community of Carmacks. Data used here are from Water Survey of Canada (2023a).

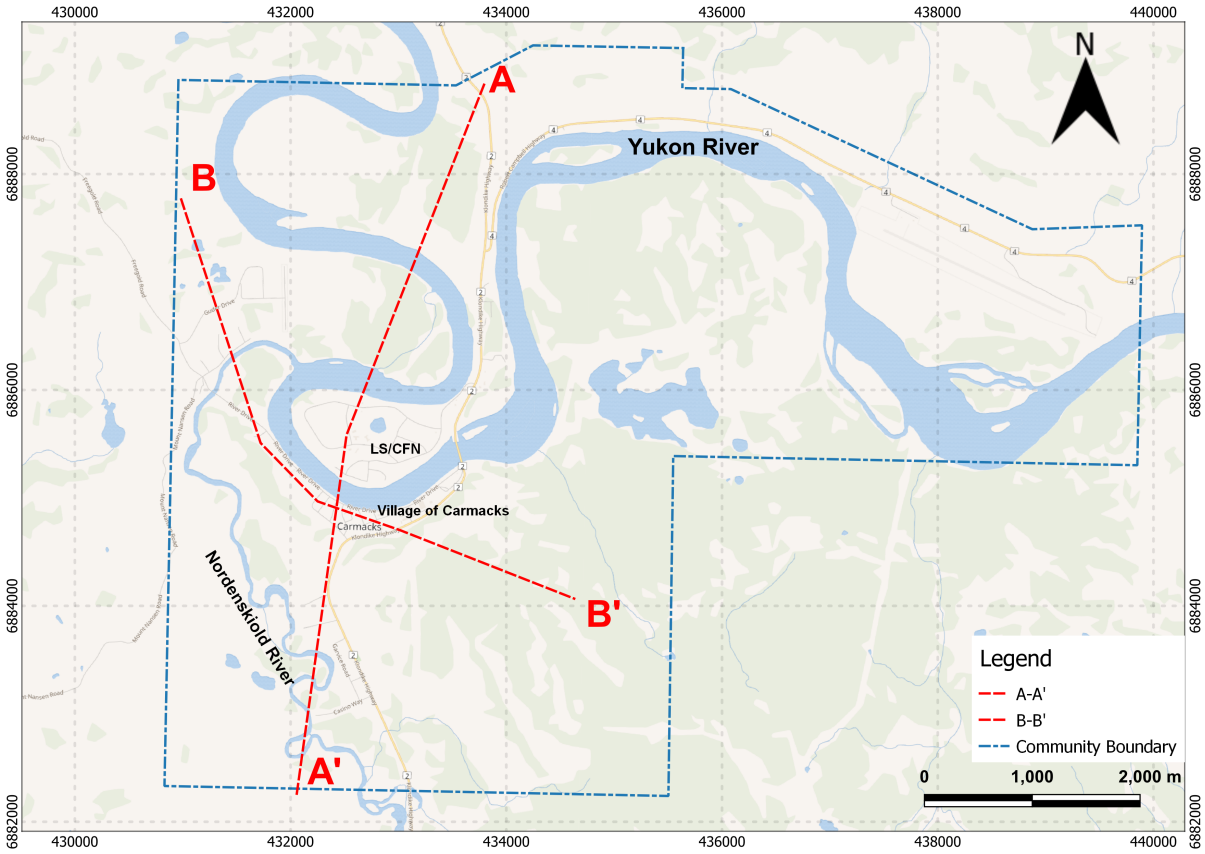

Figure 4. A plan view map shows the location of cross-section diagrams (A-A' and B-B') that demonstrate the hydrostratigraphic information of the community of Carmacks. Background map data: © OpenStreetMap (2023).

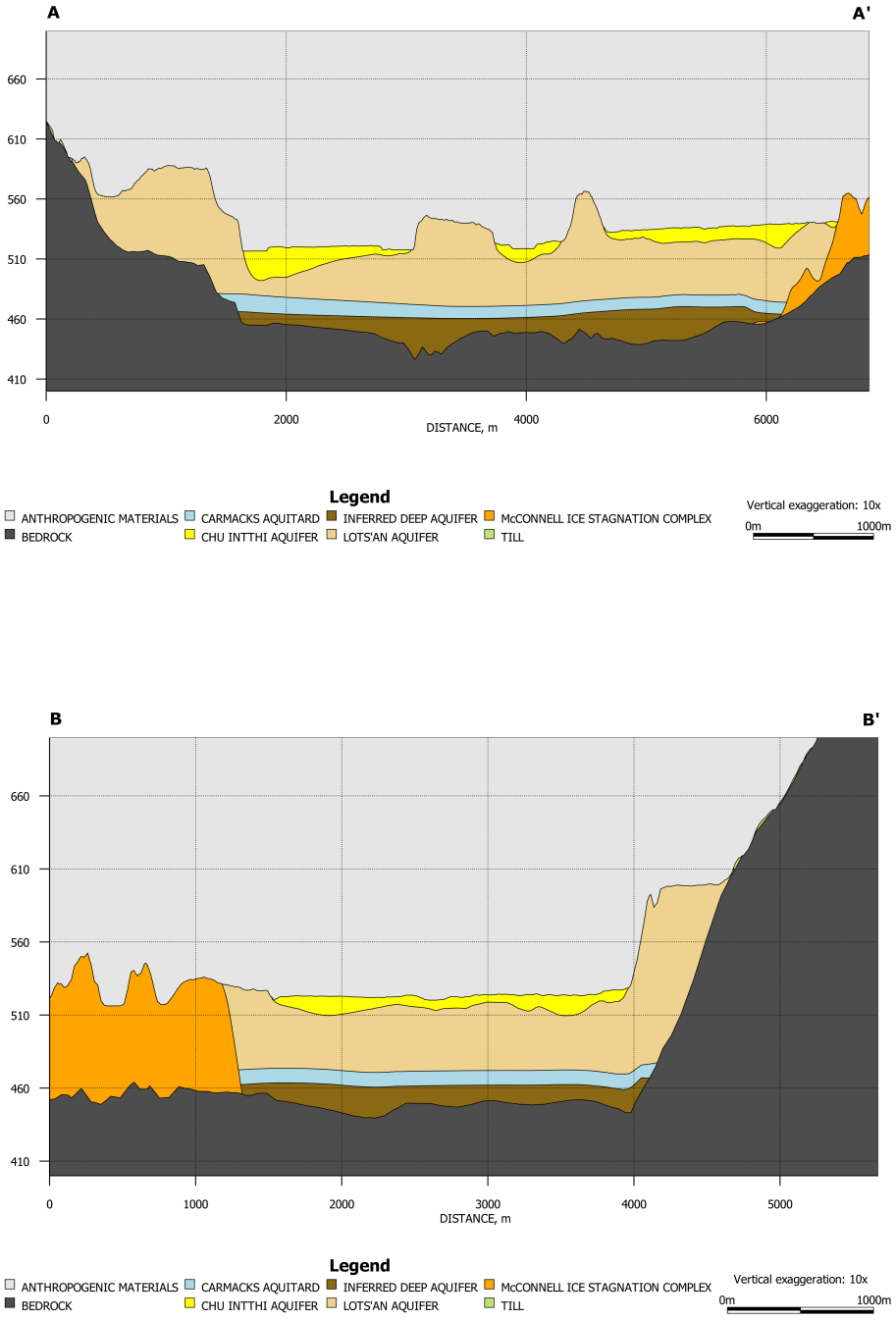

Figure 5. Hydrostratigraphic cross-section diagrams along A-A' and B-B'. (Data used to produce the cross-section diagrams were adapted from Golder Associates, 2021).

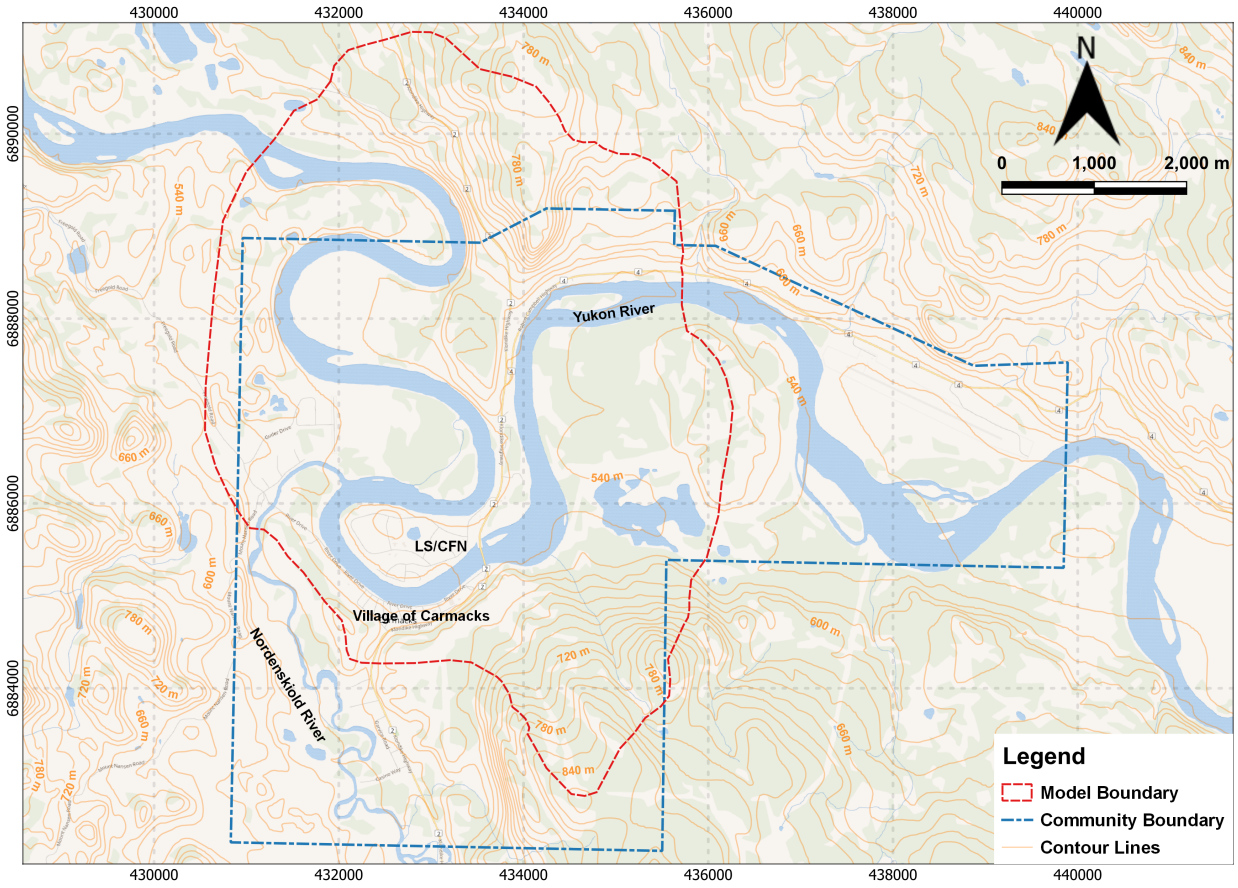

Figure 6. A map shows the Carmacks community boundary, the numerical model boundary, and ground surface contour lines with a 20-m interval. Background map data: © OpenStreetMap (2023). Topographic map data from Government of Yukon (2022b).

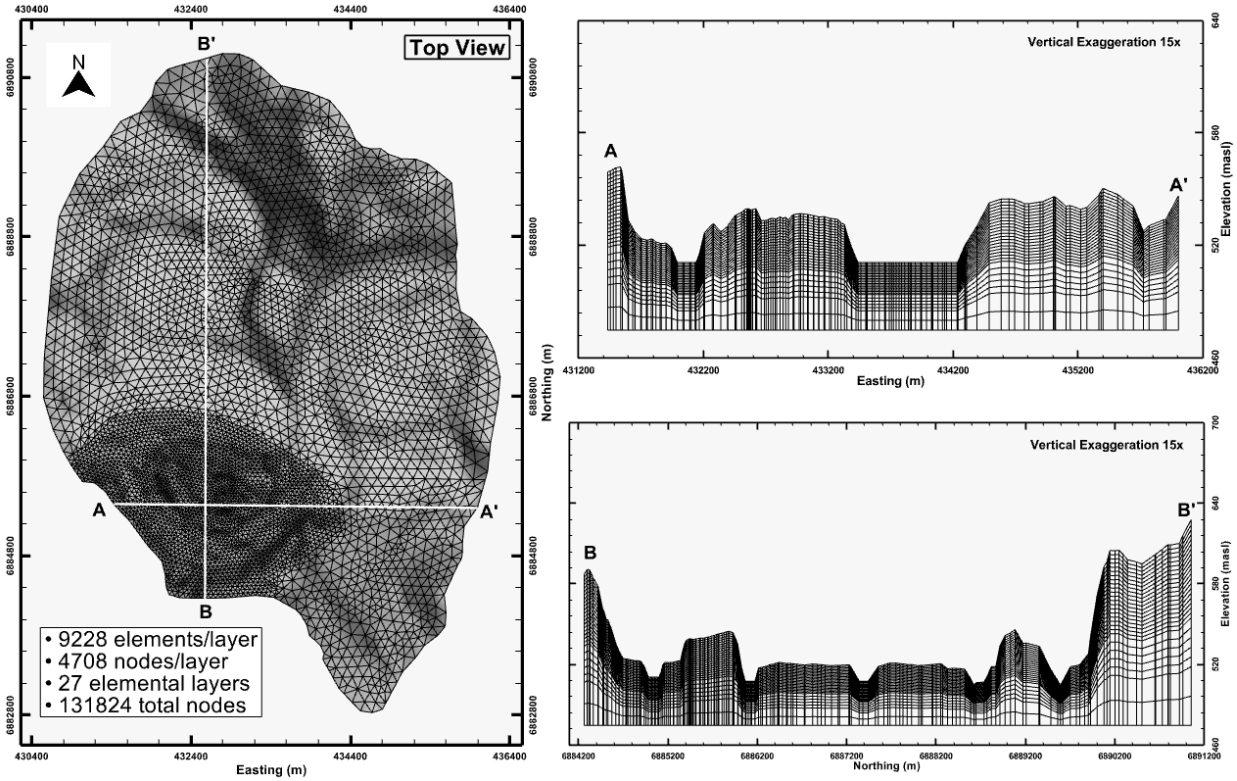

Figure 7. Discretized conceptual model showing the plan view and two cross sections. The locations of the cross sections are noted on the plan view diagram.

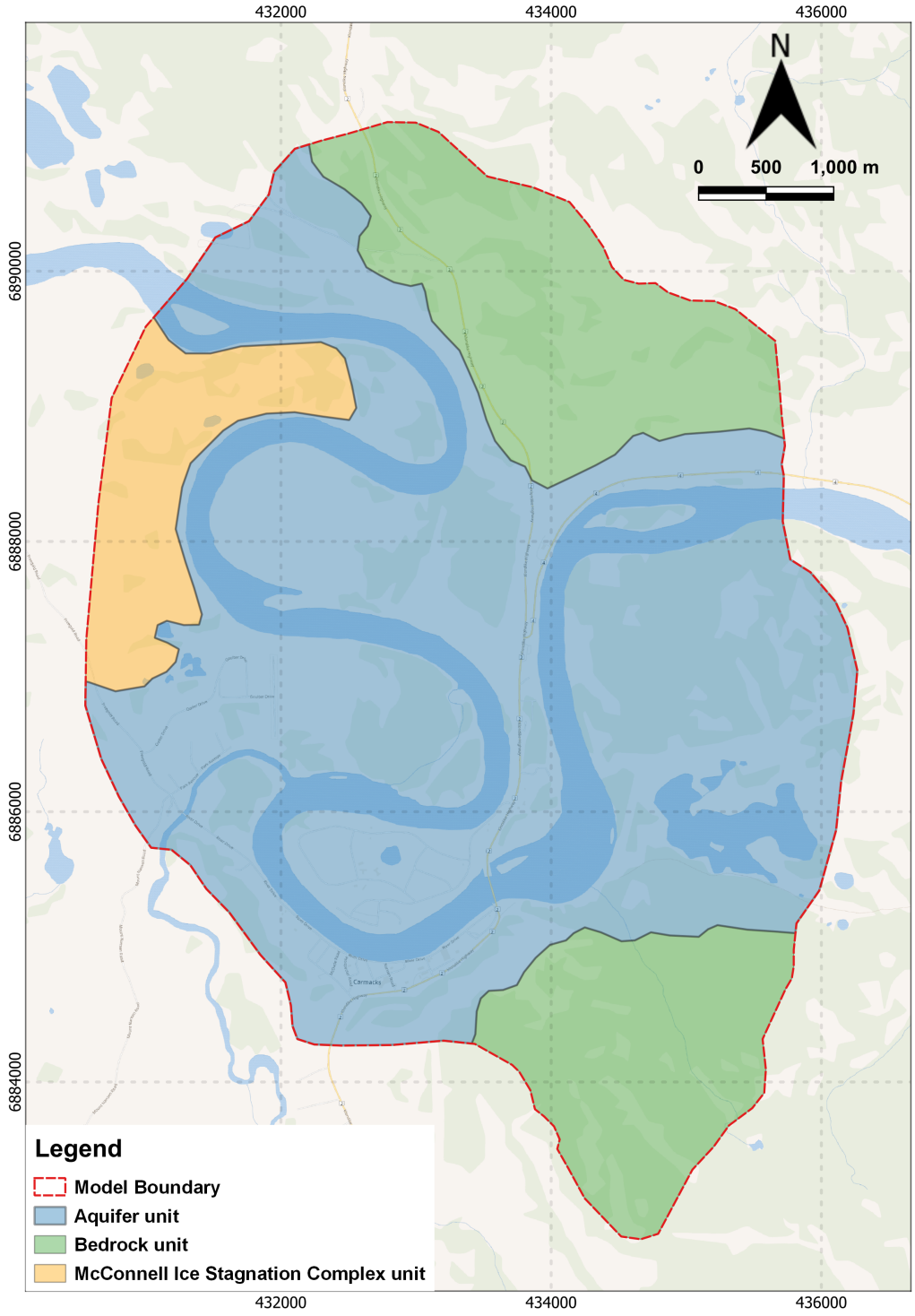

Figure 8. A plan view map shows the distribution and extent of geological units in the porous media domain. Background map data: © OpenStreetMap (2023).

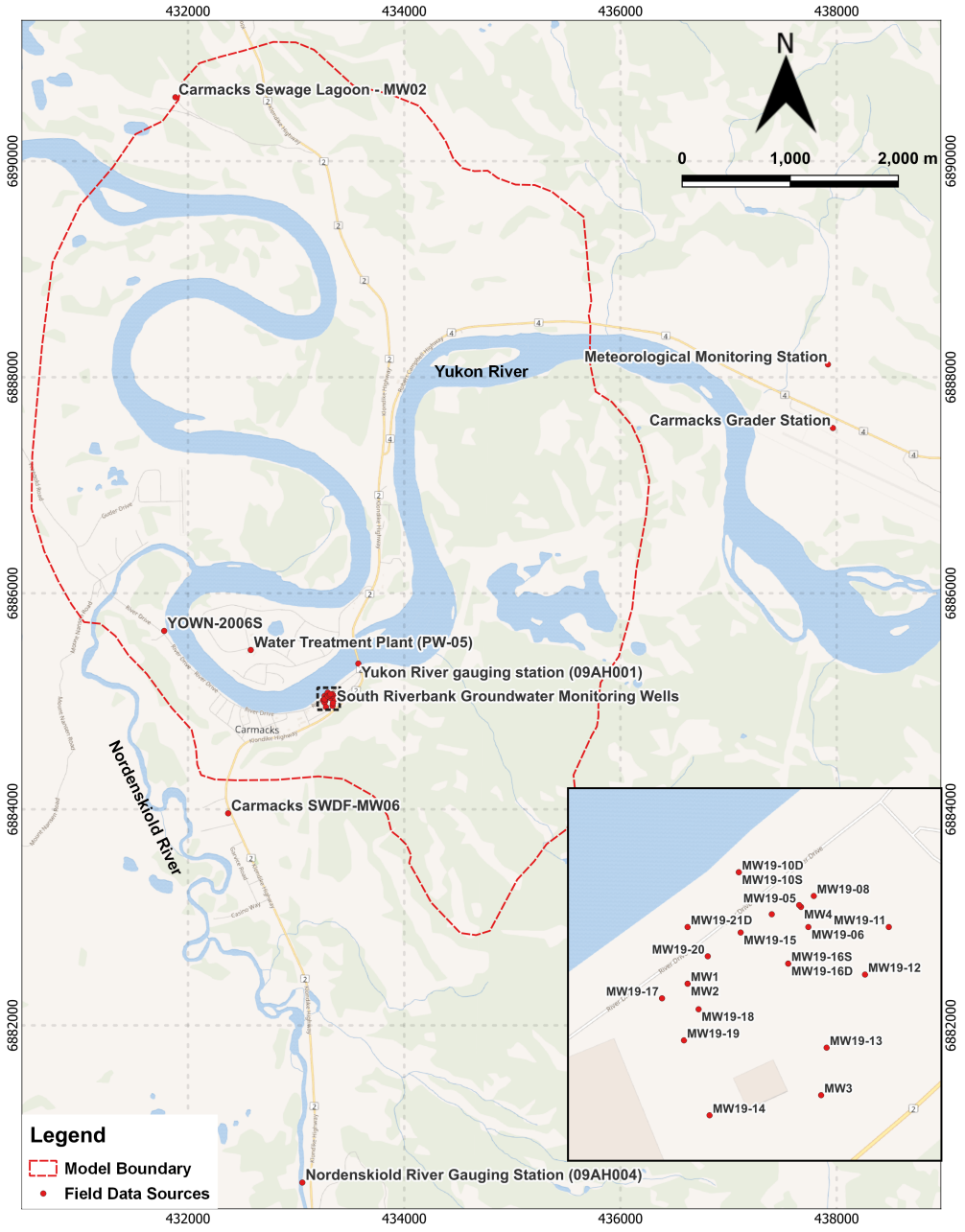

Figure 9. A plan view map shows the locations of field data collection points. The inset map demonstrates the detailed information on the South Riverbank Groundwater Monitoring Wells in the dashed black box. The collected data from these collection points were used to assign model properties and boundary conditions and used for model calibration. Background map data: © OpenStreetMap (2023).

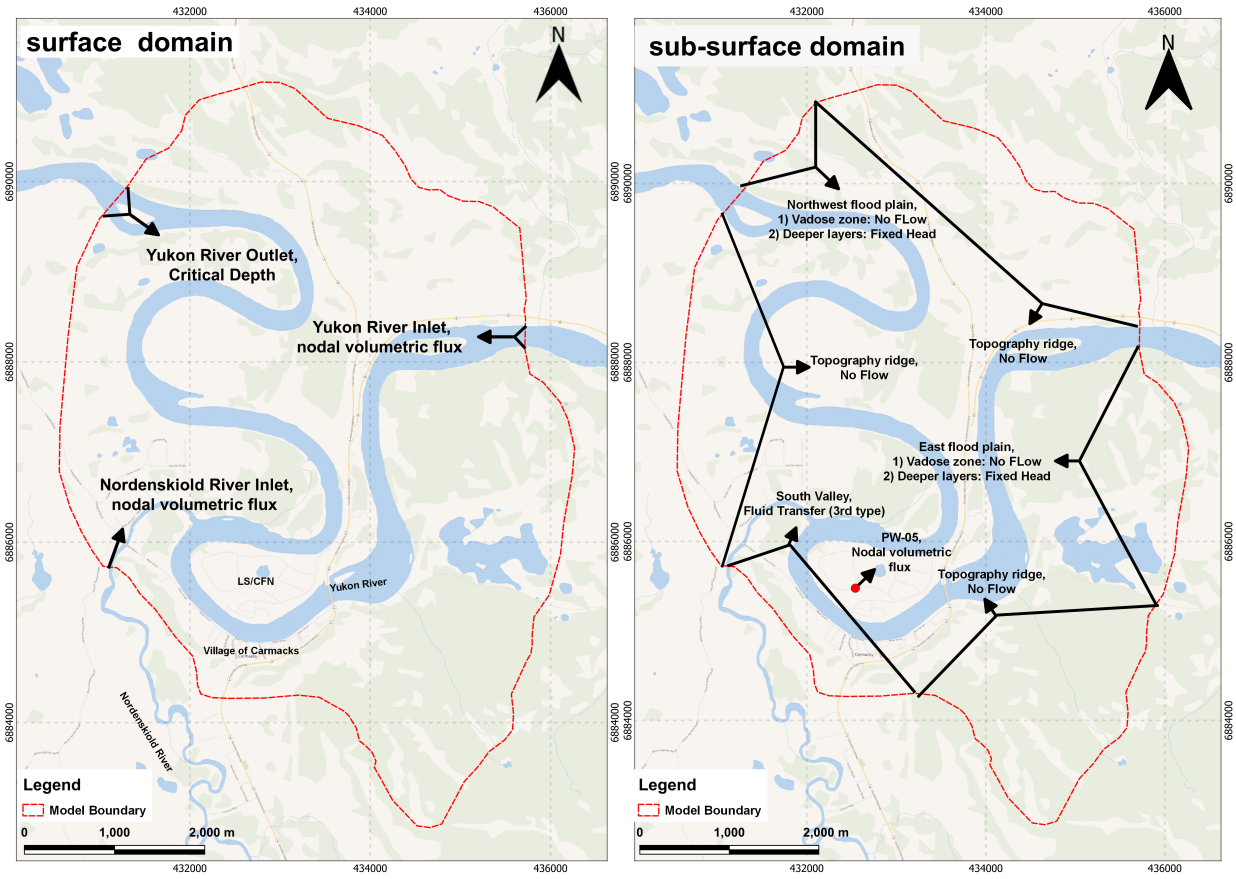

Figure 10. Model boundary conditions illustration. The red dot, black brackets and arrows in the surface domain (left) and the sub-surface domain (right) indicate where the boundary conditions are assigned. The text next to each arrow explains the type of assigned boundary condition. Background map data: © OpenStreetMap (2023).

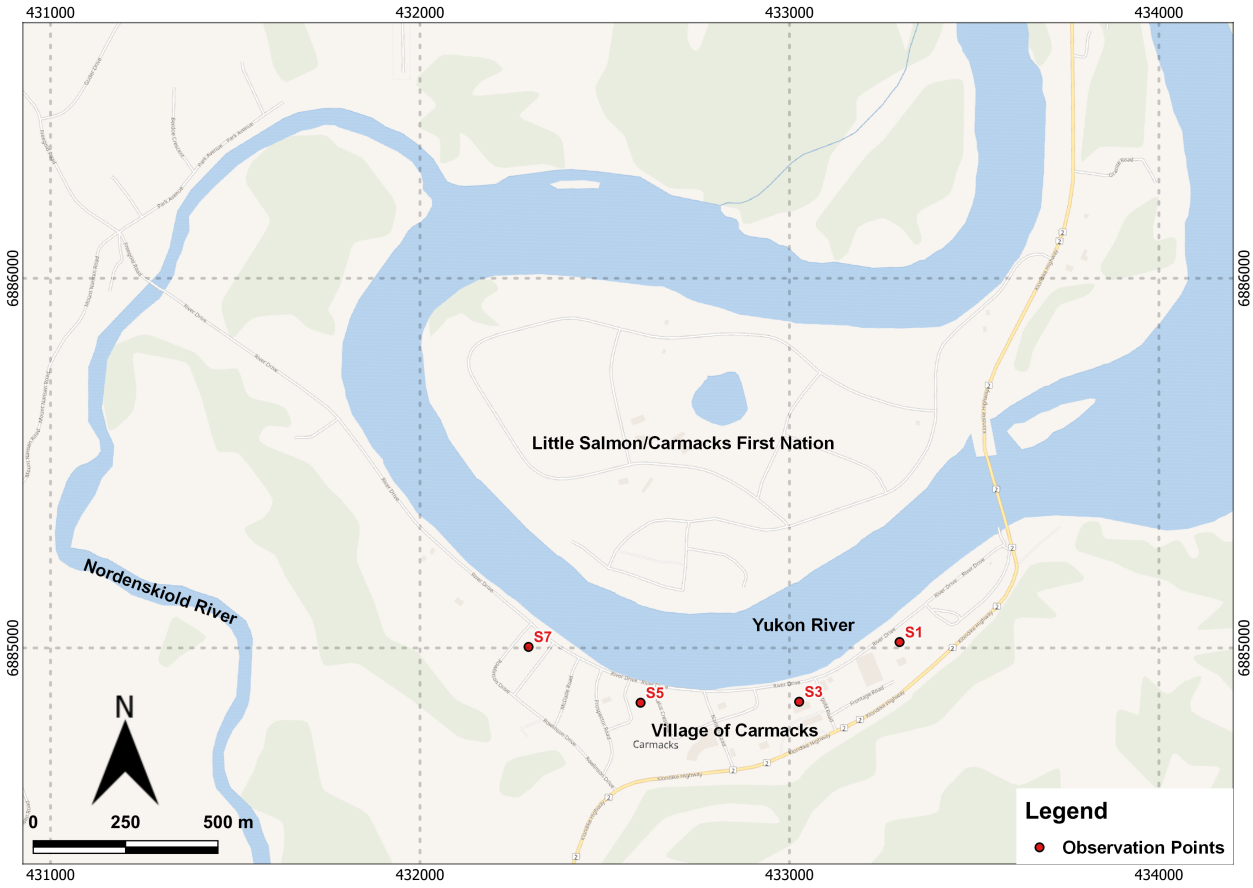

Figure 11. A map shows the locations of observation points, which are manually placed within the numerical model and used to extract model simulation results for household basement inundation analyses. Background map data: © OpenStreetMap (2023).

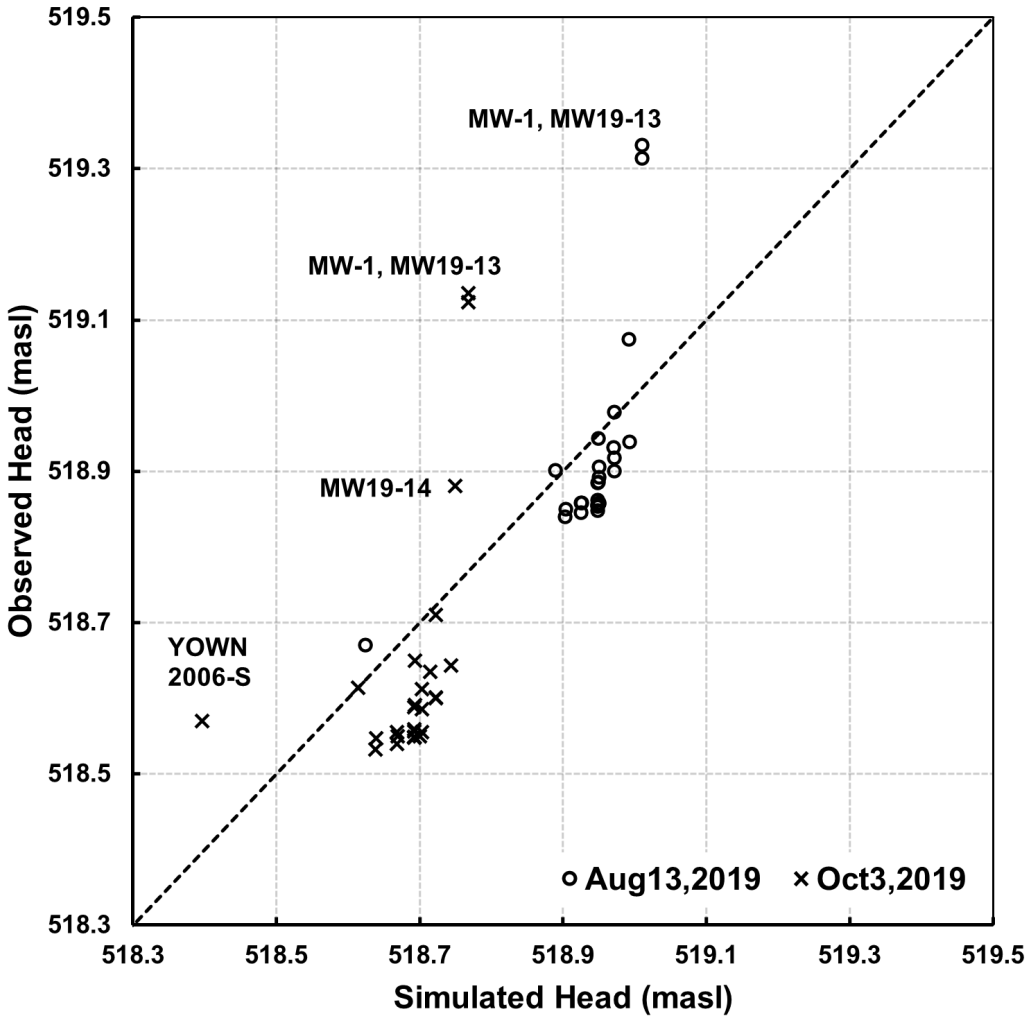

Figure 12. Model calibration results illustrating the agreement between field monitored hydraulic head data collected at the field site in August and October, 2019.

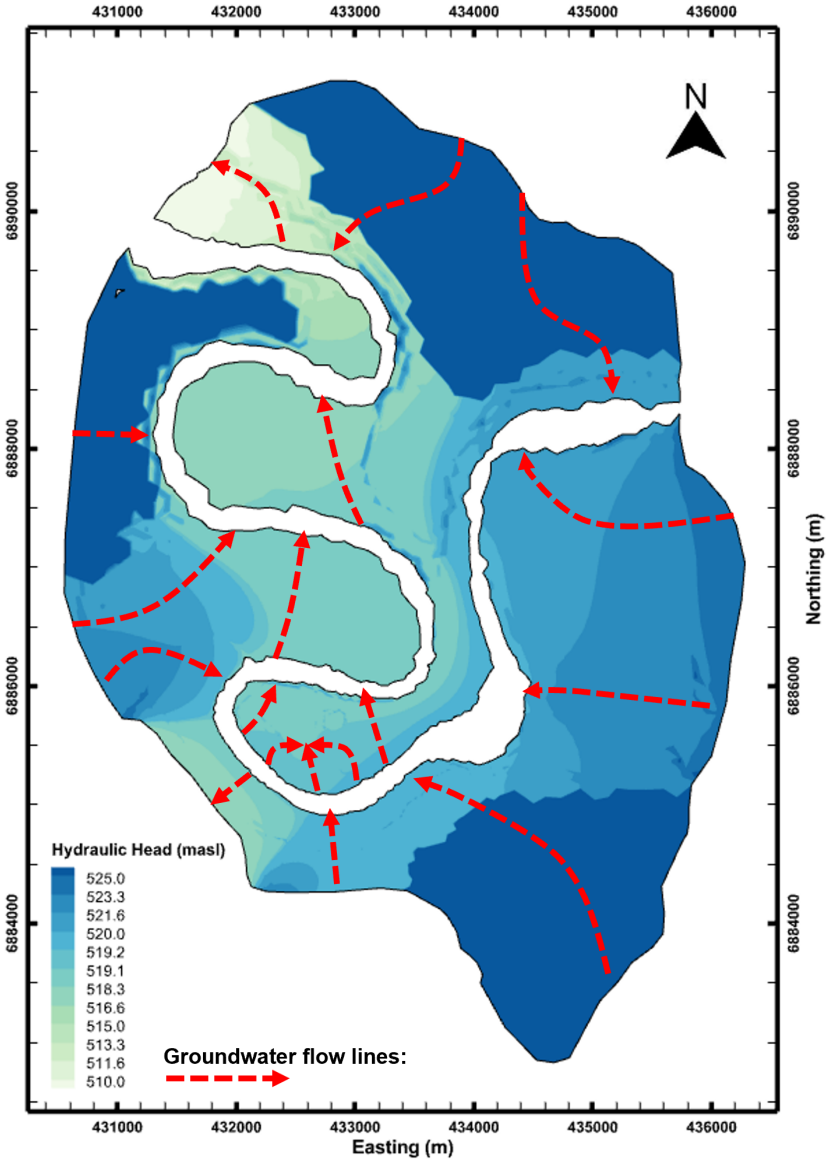

Figure 13. Simulated hydraulic head in the porous media domain under the base case scenario. Red dashed lines represent the regional groundwater flow direction.

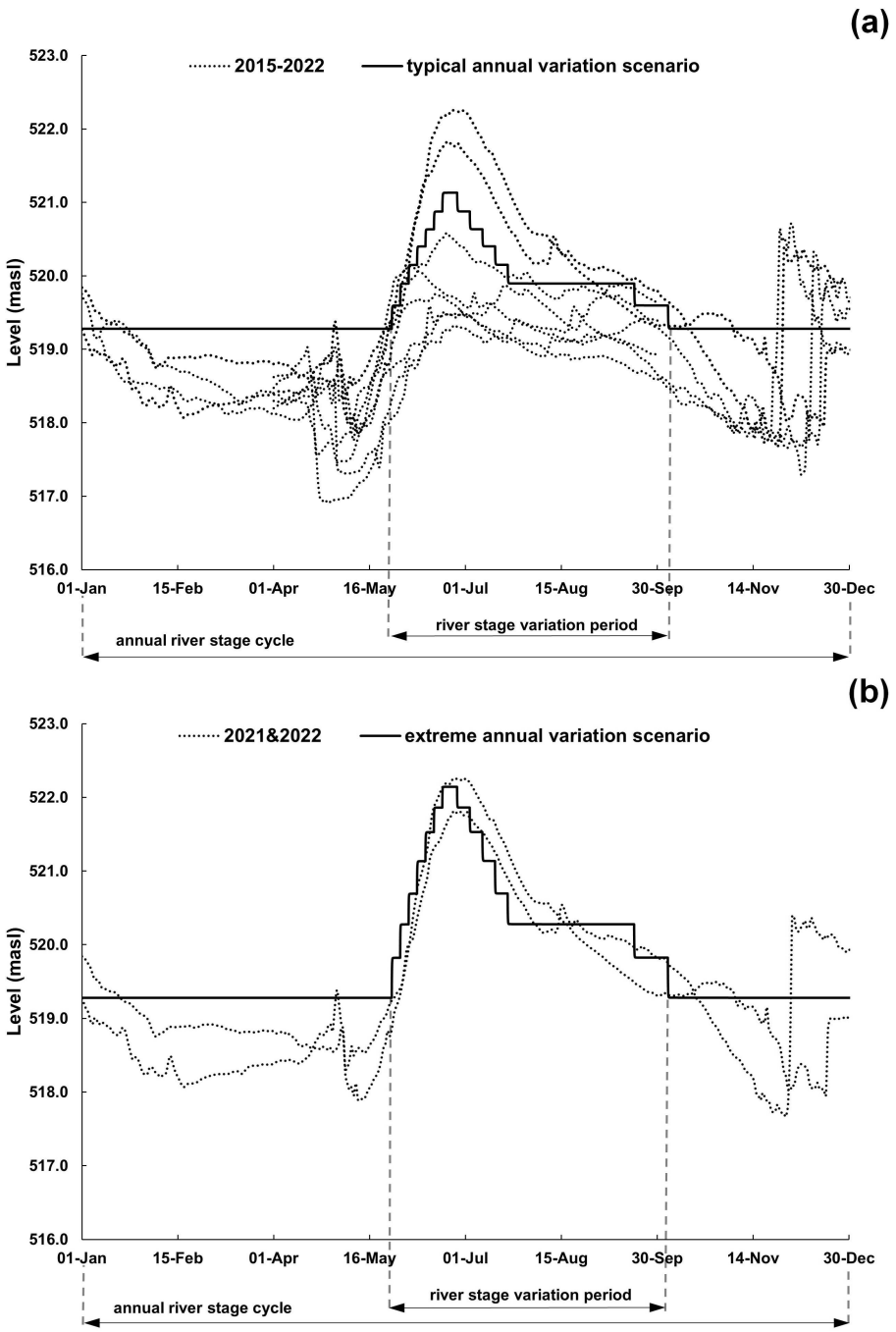

Figure 14. Simulated annual river stage cycle in the (a) typical annual variation scenario, and (b) extreme annual variation scenario. The solid black line represents the simulated river stage and the dotted lines represent the measured historical river stage. Data used for the dashed lines are from Water Survey of Canada (2023a).

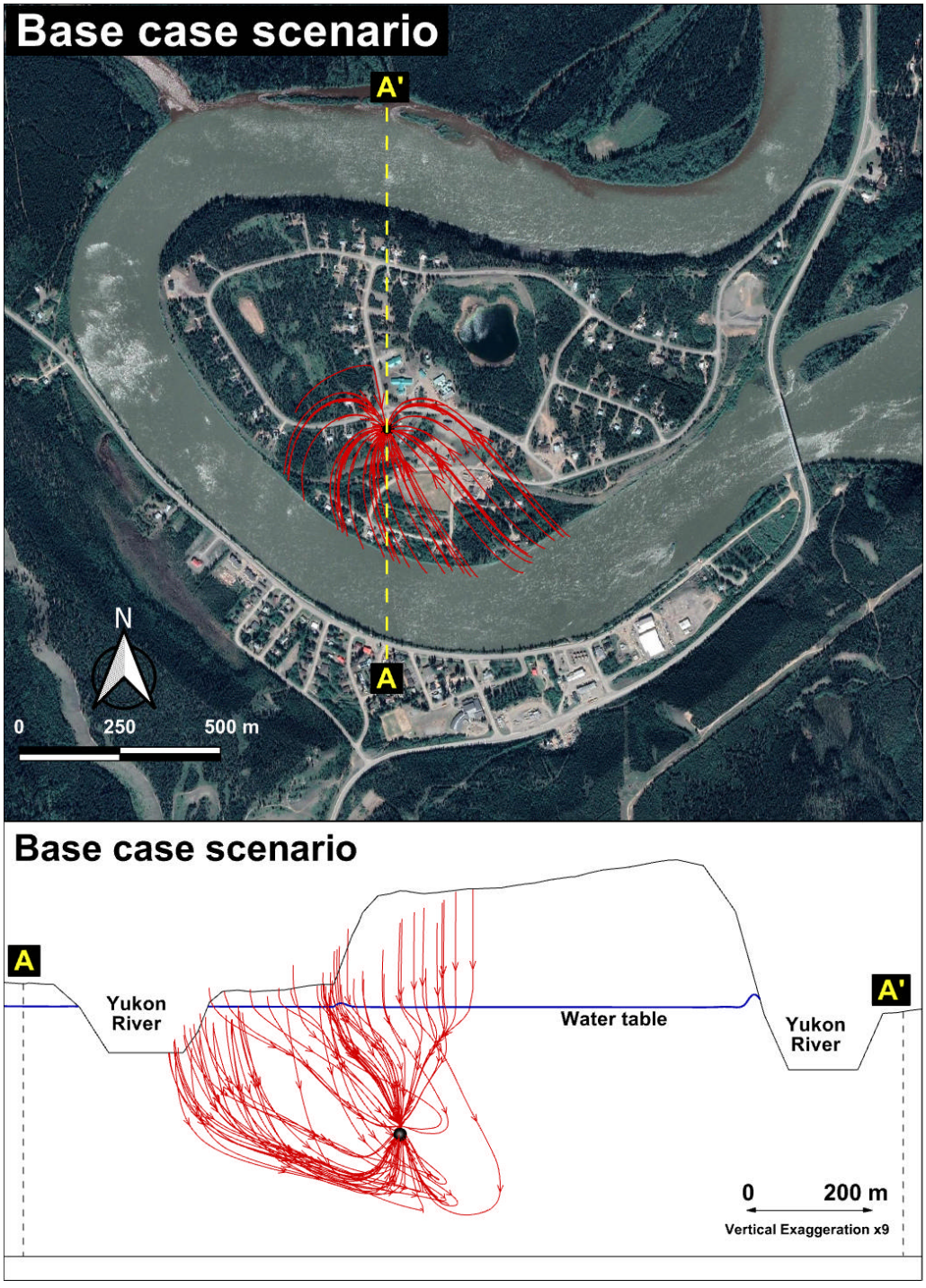

Figure 15.Streamtracing results under the base case scenario in plan view and cross-section view. The blue line in the cross-section view represents the simulated water table. Background aerial photo: © Google (2015).

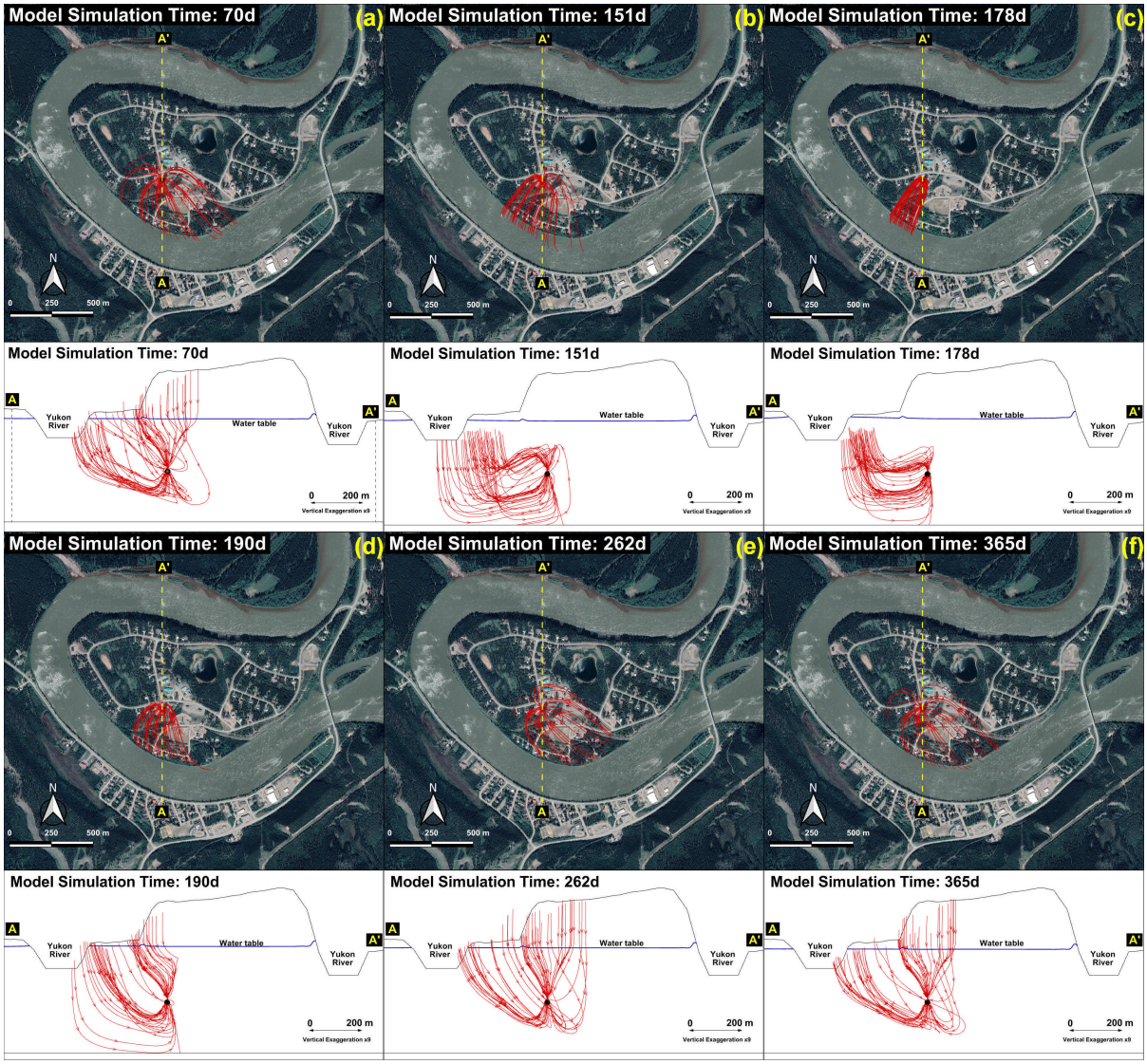

Figure 16. Streamtracing results during a river stage cycle of the typical annual variation scenario. The blue line in the cross-section view diagram represents simulated water table. Background aerial photo: © Google (2015).

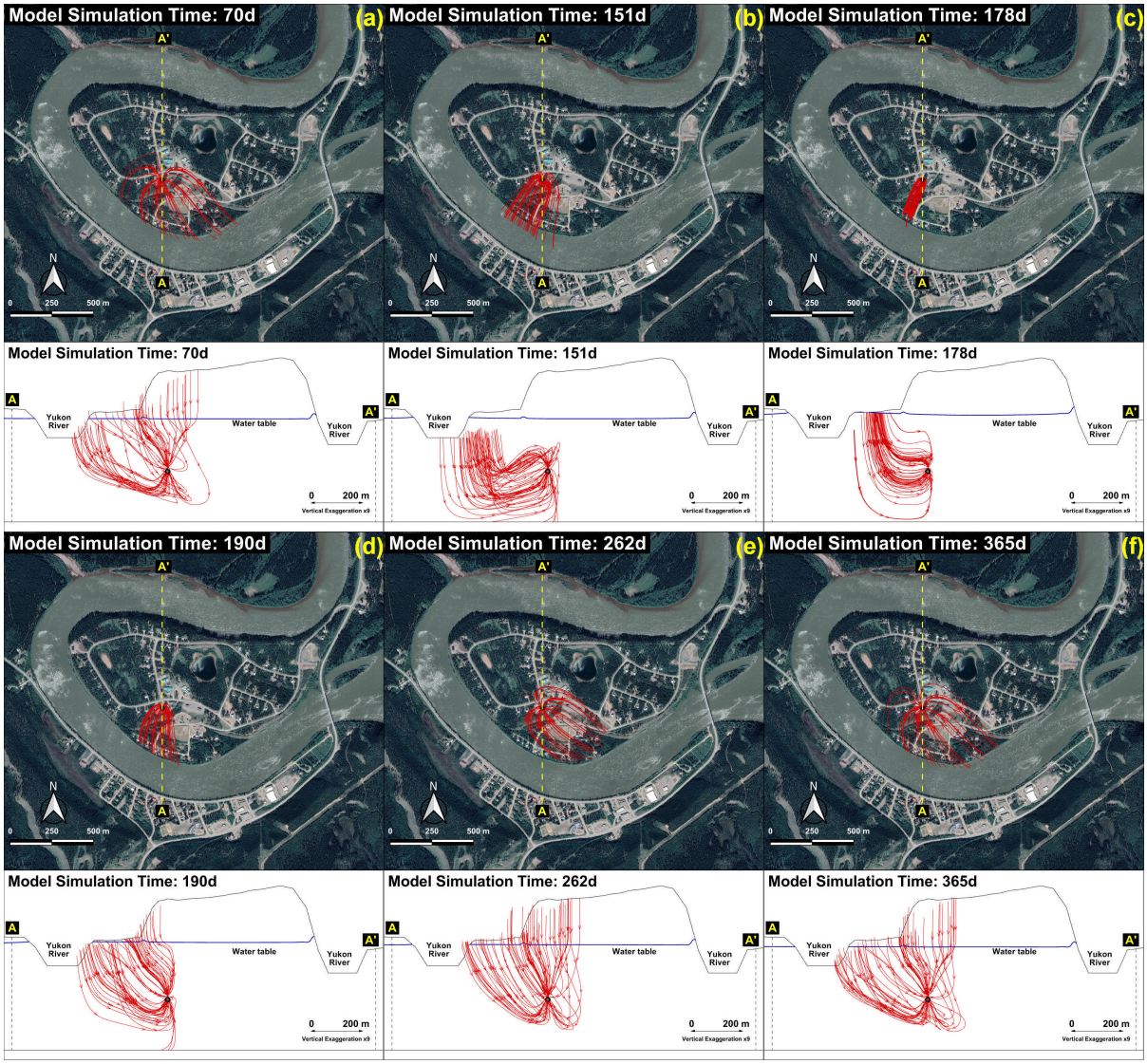

Figure 17. Streamtracing results during a river stage cycle of the extreme annual variation scenario. The blue line in the cross-section view diagram represents simulated water table. Background aerial photo: © Google (2015).

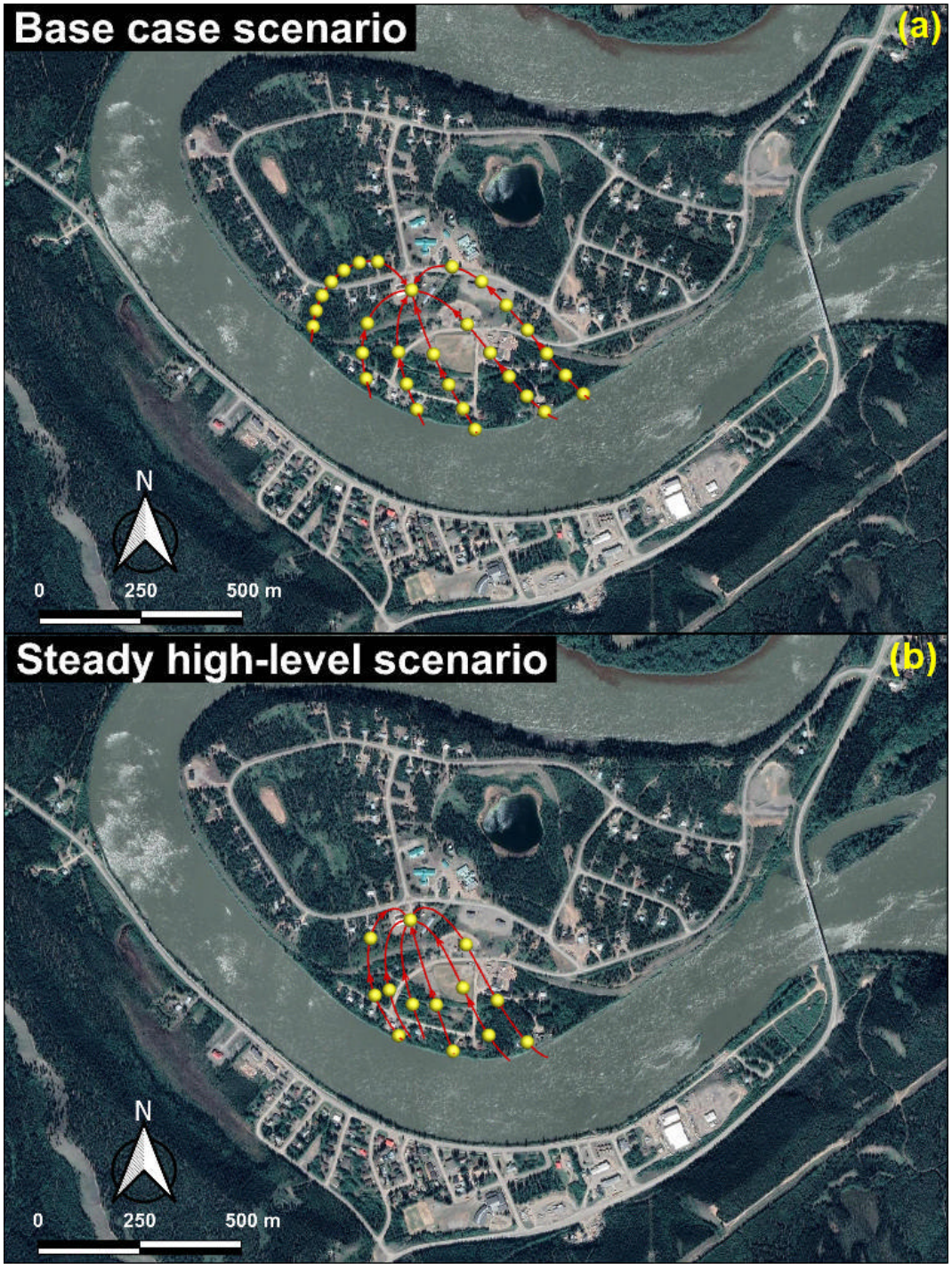

Figure 18. Stream markers results for (a) base case scenario; and (b) steady high-level scenario. The yellow spherical dots represent stream markers and the time interval between each yellow dot is ten years. Background aerial photo: © Google (2015).

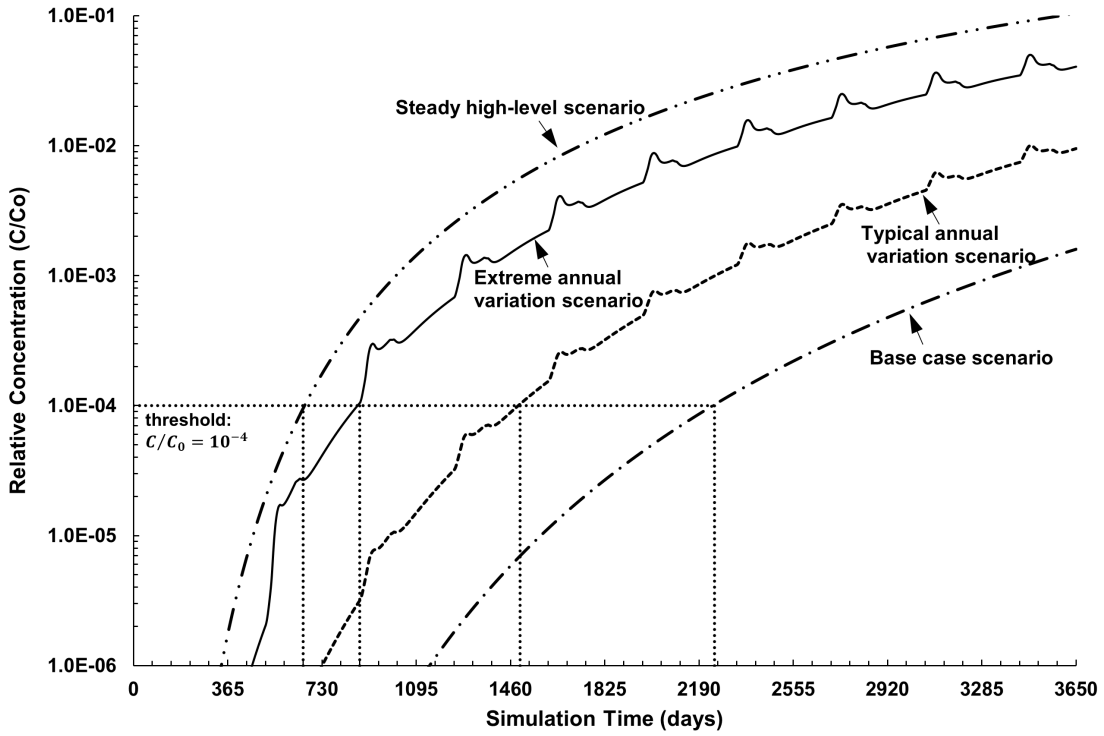

Figure 19. Solute relative concentration at PW-05 under base case scenario, steady high-level scenario, typical annual variation scenario, and extreme annual variation scenario, simulated for 10 years.

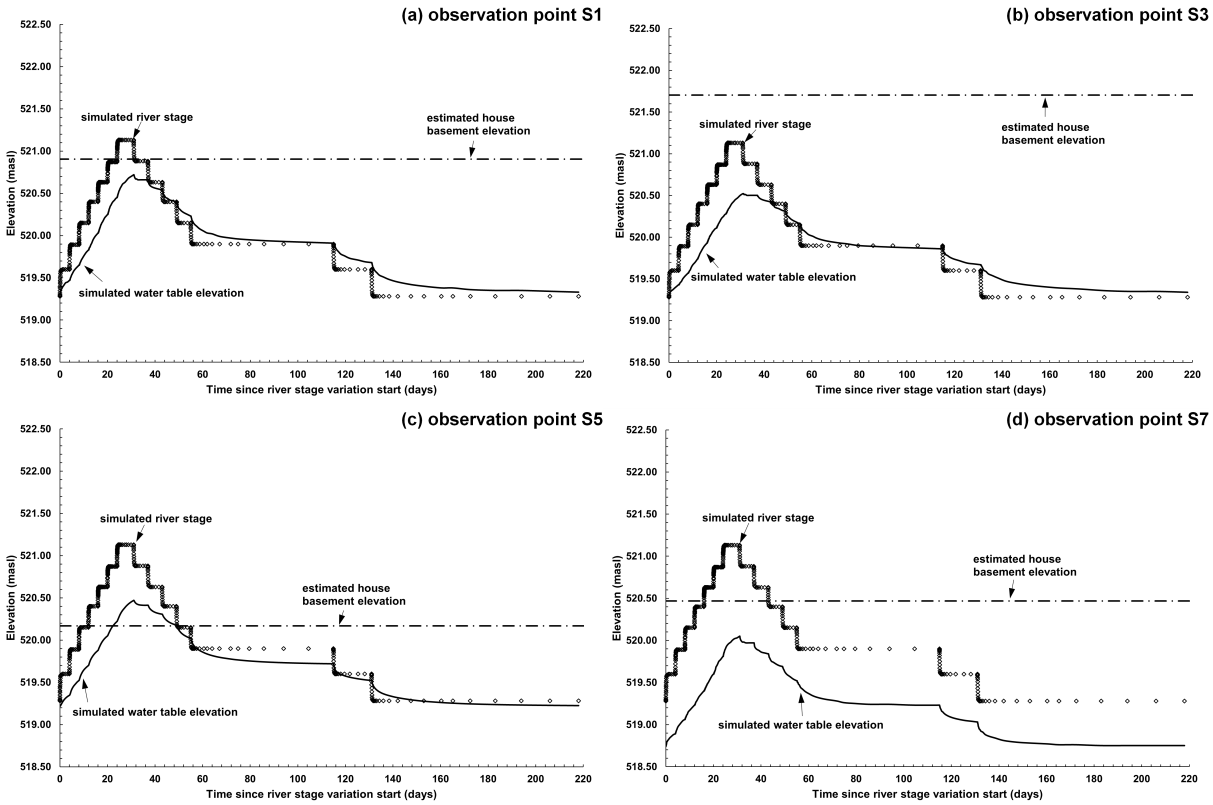

Figure 20. Plots showing estimated basement elevation and simulated water table at four observation points (S1, S3, S5, and S7) during a typical river stage variation. The simulated river stage at the Yukon River gauging station was also added.

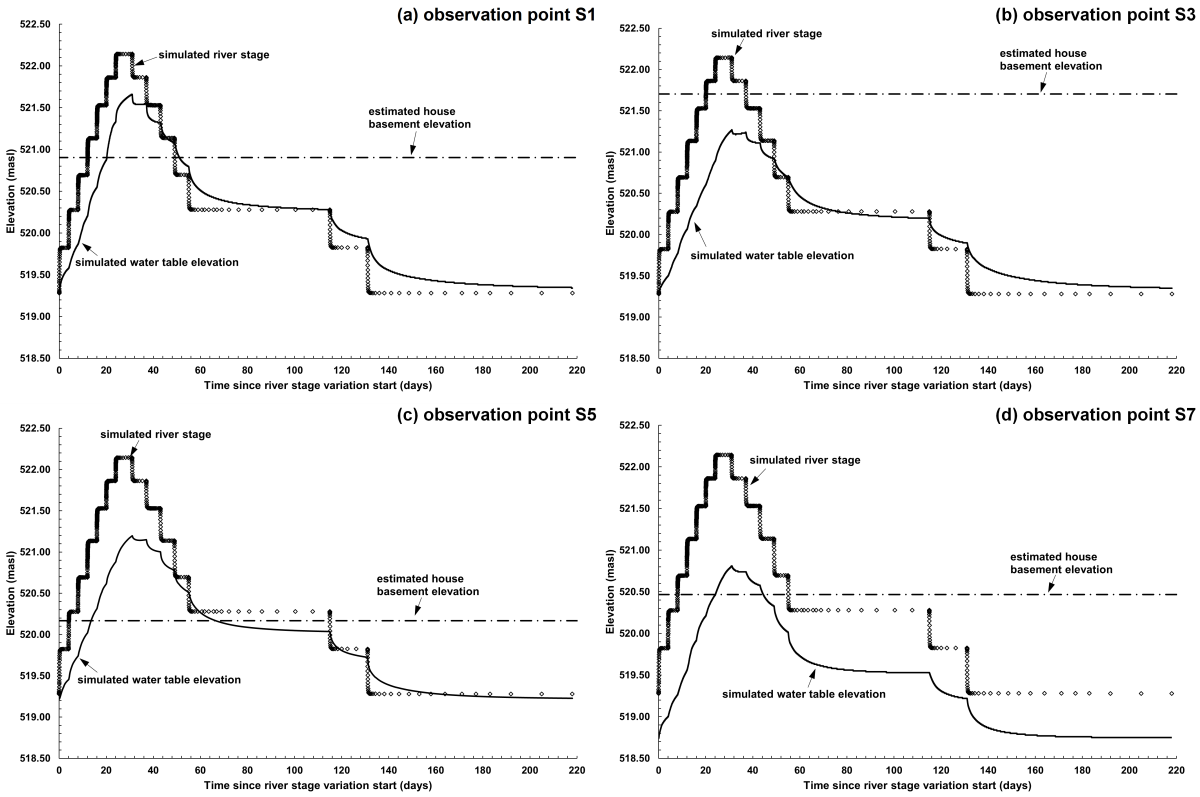

Figure 21. Plots showing estimated basement elevation and simulated water table at four observation points (a) S1, (b) S3, (c) S5, and (d) S7 during an extreme river stage variation. The simulated river stage at the Yukon River gauging station was also added.

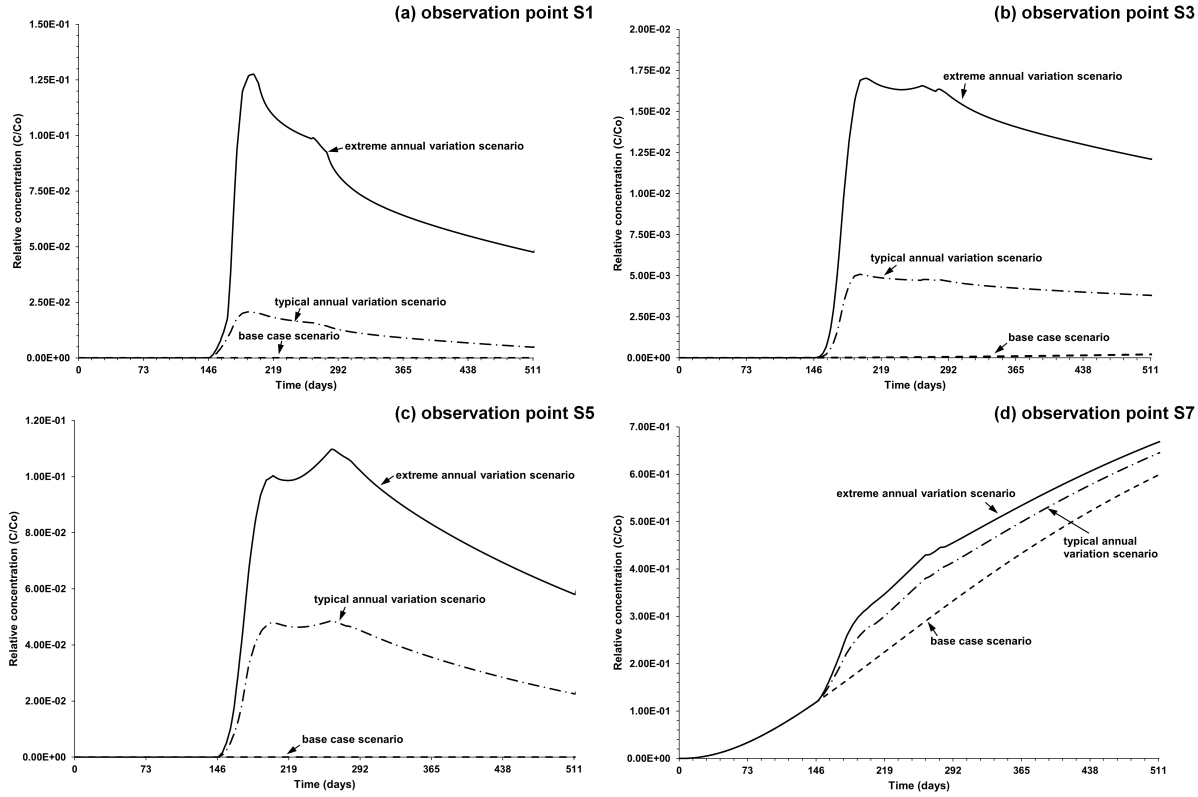

Figure 22. Plots showing the breakthrough curves of four observation points along the riverbank: (a) S1, (b) S3, (c) S5, and (d) S7 under the base case scenario, the typical annual variation scenario, and the extreme annual variation scenario.

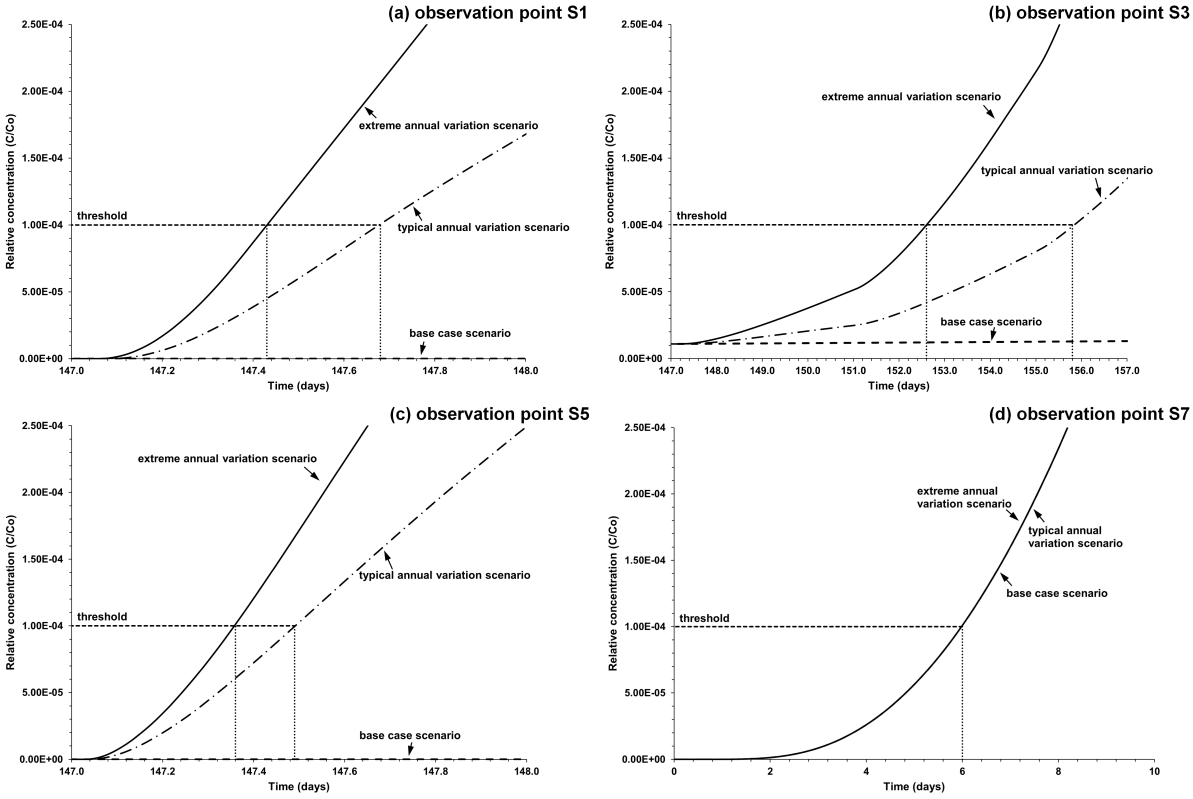

Figure 23. Plots showing the rapid increase of relative concentration at observation points S1 (a), S3 (b), and S5 (c) since the river stage variation period start, and the rapid increase of relative concentration at S7 (d) since the simulation start. A threshold level (10^{-4}) is added to each plot for examining the "arriving time" under different scenarios.

Figure 24. Location of two cross-section diagrams: B-B' and C-C'. Background aerial photo: © Google (2015).

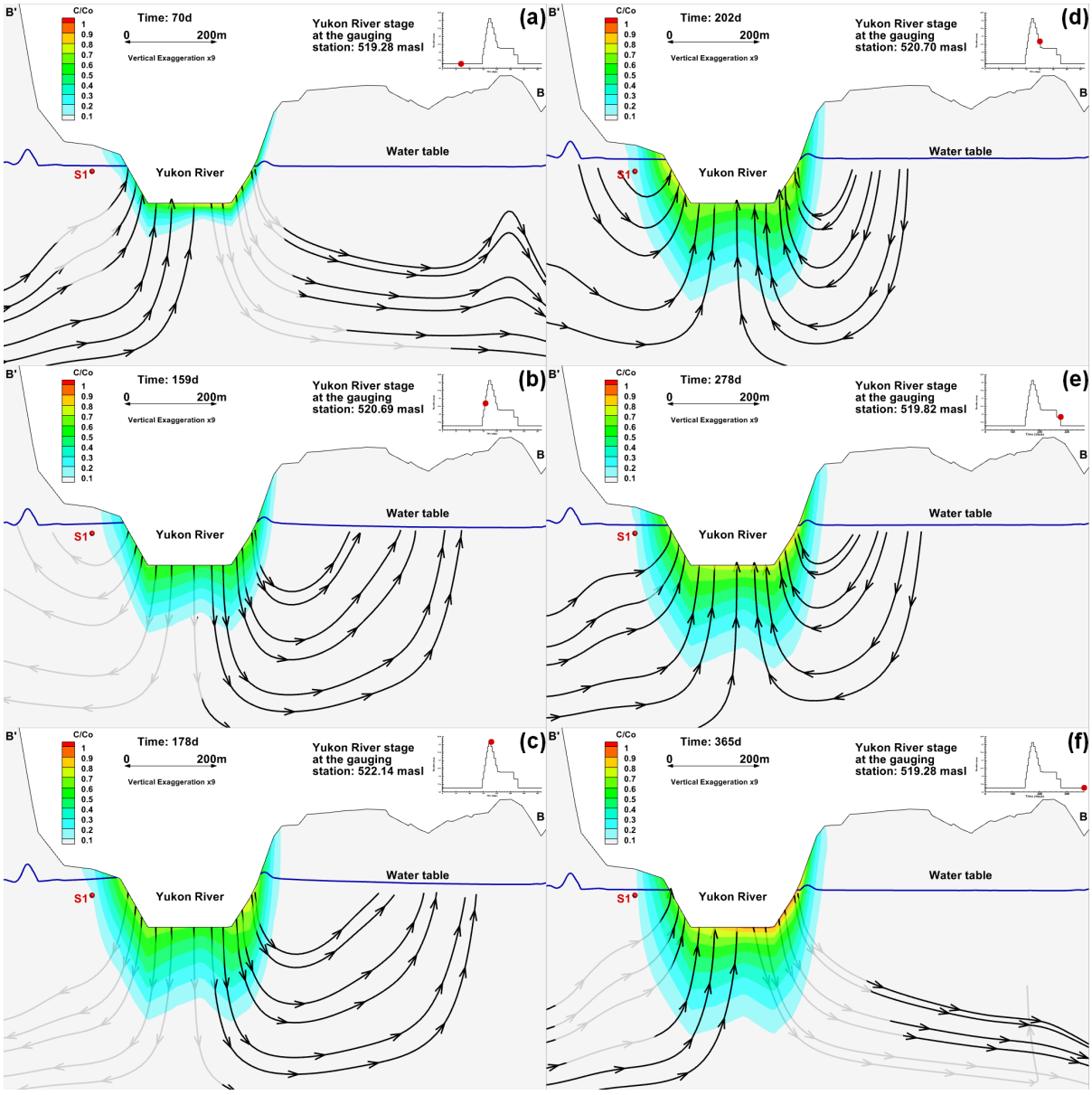

Figure 25. Cross-section diagrams showing the water table, groundwater flow direction (black lines with arrows), and the river-origin solute migration at B-B' during the first annual river stage cycle of the extreme annual variation scenario. An inset plot indicates the current river stage along the annual river stage cycle in each sub-diagram. The location of the observation S1 is also illustrated.

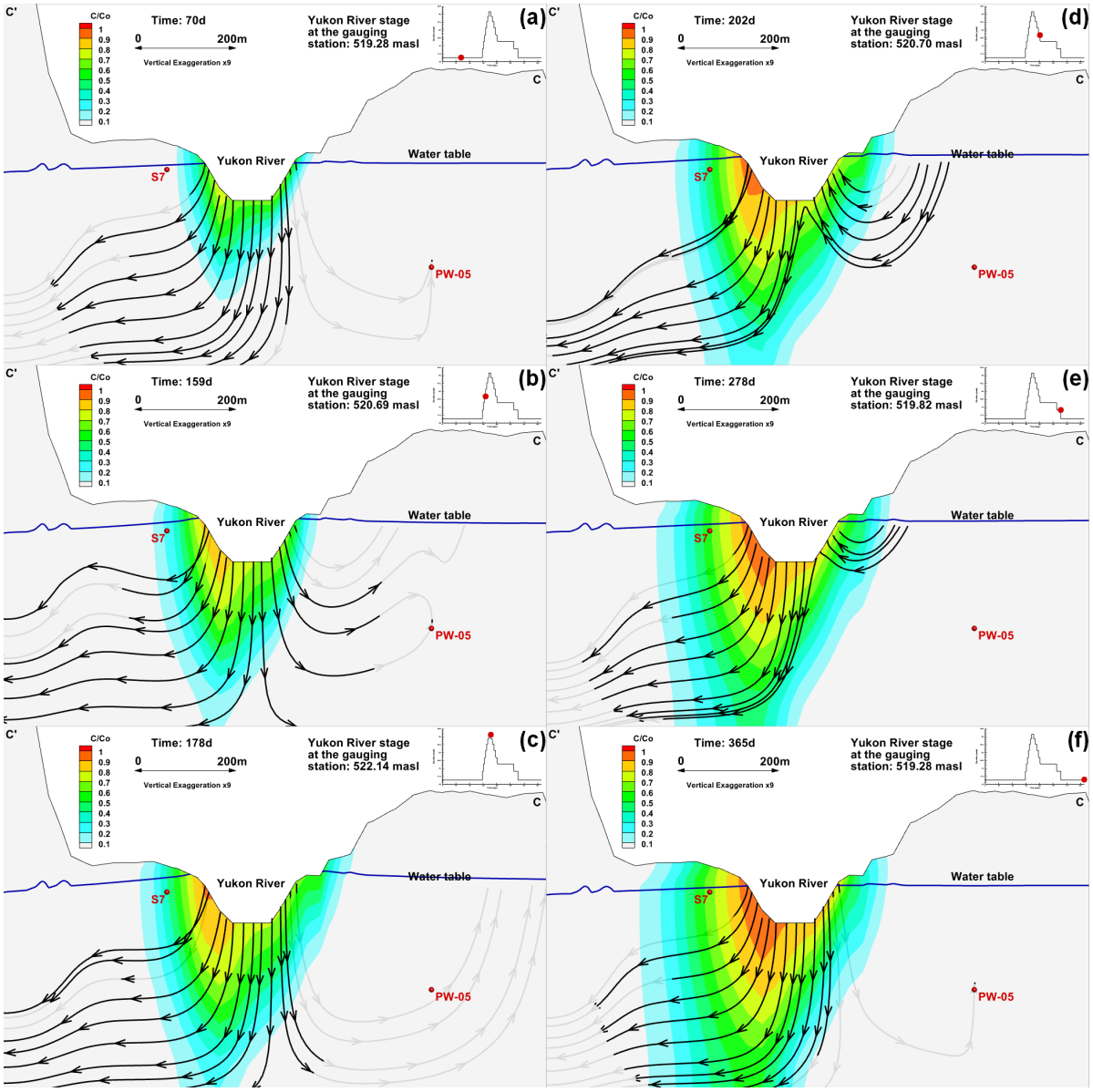

Figure 26. Cross-section diagrams showing the water table, groundwater flow direction (black lines with arrows), and the river-origin solute migration at C-C' during the first annual river stage cycle of the extreme annual variation scenario. An inset plot indicates the current river stage along the annual river stage cycle in each sub-diagram. The locations of observation point S7 and the water supply well PW-05 are also illustrated.

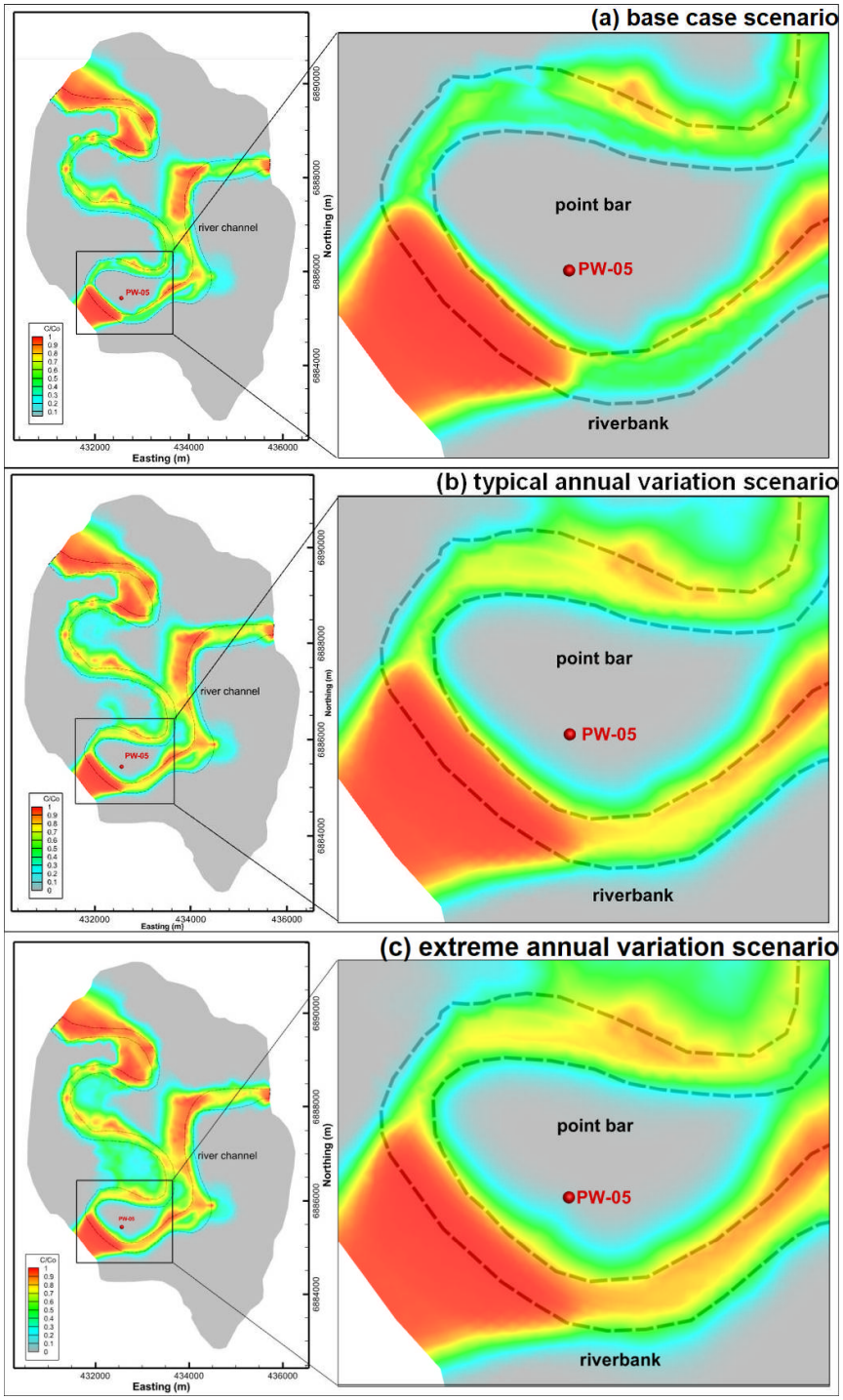

Figure 27. Solute transport simulation results in porous media at t = 10 years under: a) base case scenario, b) typical annual variation scenario, and c) extreme annual variation.

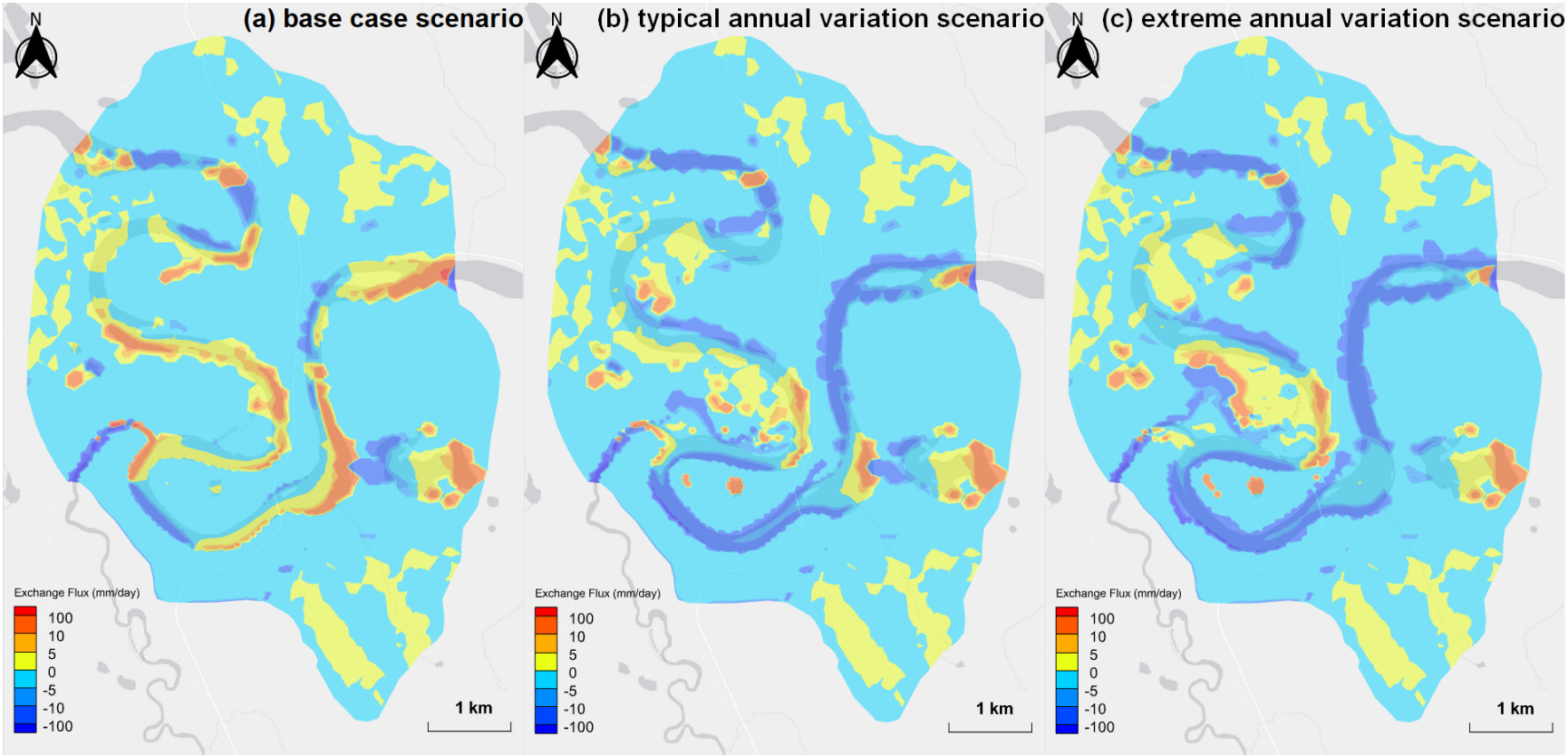

Figure 28. Simulated exchange flux (mm/day) between the surface domain and sub-surface domain under base case scenario (a), and typical annual variation scenario (b) and extreme annual variation scenario (c) when river stage peaks within an annual river stage cycle (time= 178 day). A base map is inserted into each plot to indicate the location of river channel of Yukon River and Nordenskiold River. Background map data: © Esri (2023).

Chapter 3
Conclusions and Recommendations

Overall, the thesis demonstrates that for a river-connected aquifer, the seasonal river stage variation can increase the vulnerability of water wells that have well screens constructed within the aquifer, and the magnitude of the seasonal river stage fluctuation may be a controlling factor for the occurrence of house basement inundation issues. In addition, the case study demonstrates the necessity of employing transient model scenarios that incorporate river stage changes instead of relying on a simple steady state model when evaluating well vulnerability. These conclusions are based on five key findings from the case study in Chapter 2:

1) The case study shows that variation in the river stage could temporarily change the groundwater flow direction within an aquifer, inducing shifts in the orientation and extent of the area that contributes groundwater to the pumping wells.

2) The case study reveals that the seasonal river stage variation can accelerate the transport of solutes from the river to the adjacent river-connected aquifer, and the acceleration is positively related to the magnitude of the river stage variation.

3) River stage fluctuations can temporarily alter the regional groundwater-surface water interactions. A stream reach that is gaining river water before the river stage variation begins can switch to a losing stream during the river stage rising period and then switch back to gaining stream during the following river stage recession period. This switching of groundwater-surface water interaction facilitates the spreading of river-origin solute into the riverbank.

4) It was found that the river stage variation in the extreme annual variation scenario caused basement inundation problems for more households along the riverbank compared to the typical annual variation scenario.

5) The numerical model with transient scenarios can reproduce the dynamics of groundwater-surface water interactions under fluctuating river stage, which is the “bank storage” process and the “flush-out” process. However, a steady state scenario omits the “flush-out” process

and indicates a biased solute migration simulation result, which can mislead well vulnerability assessment.

While the case study was conducted in one community in the central Yukon, Canada, the key finds and conclusions from this research can also make contributions and be transferred to other communities in Northern Canada and other cold regions where the challenges and the hydrogeological environment are similar to what has been discussed in the case study. The exact field situations can vary from one community to the other, which means the presented model and methods used to evaluate the well vulnerability and basement inundation issues might need adjustment. The following recommendations might be considered for further research and while applying the research outcomes in other communities:

1) Although the numerical model was carefully designed and calibrated, as discussed previously in the thesis, to reproduce the field situations, the case study ignores the heterogeneity of geological units due to the limited available field data at the study site. Future field work such as testing hydraulic conductivities and investigating subsurface stratigraphy information at more locations within the study area could improve the understanding of the extent and heterogeneity of different geological units, which are lacking in the presented numerical model.

2) The case study applied a relative concentration level as a threshold while evaluating the well vulnerability. This threshold level can be adjusted depending on the type of contaminants in surface water bodies.

3) For communities in Northern Canada close to rivers with seasonal river stage variation, continuously monitoring river stages and water table elevations along the riverbank may help to understand the dynamic interactions between the river and the adjacent aquifer while the river stage is fluctuating. This can help identify what locations along the riverbank are more likely to be replenished by river water, thus more vulnerable to surface water contaminants.

4) Transient scenarios should be incorporated when using a numerical model to evaluate aquifer and well vulnerability. Though transient scenarios would increase computational efforts, maintaining the accuracy of the simulation results is also critical.

References

Abboud, J. M., Ryan, M. C., & Osborn, G. D. (2018). Groundwater flooding in a river-connected alluvial aquifer. *Journal of Flood Risk Management*, *11*(4), e12334–n/a. https://doi.org/10.1111/jfr3.12334

Aller, L., Bennett, T., Lehr, J. H., Petty, R. J., & Hackett, G. (1987). *DRASTIC: A standardized system for evaluating ground water pollution potential using hydrogeologic settings*. Robert S. Kerr Environmental Research Laboratory, Office of Research and Development, US Environmental Protection Agency. https://nepis.epa.gov/Exe/ZyPURL.cgi?Dockey=20007KU4.txt

Aquanty Inc. (2015). *HGS Reference Manual* (Version 2531) [Manual]. Aquanty Inc. https://www.aquanty.com/hgs-download

Aquanty Inc. (2015). *HGS Theory Manual* (Version 2531) [Manual]. Aquanty Inc. https://www.aquanty.com/hgs-download

Barry, F., Ophori, D., Hoffman, J., & Canace, R. (2009). Groundwater flow and capture zone analysis of the central Passaic River basin, New Jersey. *Environmental Geology*, *56*(8), 1593–1603. https://doi.org/10.1007/s00254-008-1257-5

Batu, V. (1998). *Aquifer hydraulics: a comprehensive guide to hydrogeologic data analysis*. John Wiley & Sons.

Bonnaventure, P. P., Lewkowicz, A. G., Kremer, M., & Sawada, M. C. (2012). A permafrost probability model for the southern Yukon and northern British Columbia, Canada. *Permafrost and Periglacial Processes*, *23*(1), 52–68. https://doi.org/10.1002/ppp.1733

Brabets, T. P., Wang, B., & Meade, R. H. (2000). *Environmental and hydrologic overview of the Yukon River Basin, Alaska and Canada*. U.S. Geological Survey. https://doi.org/10.3133/wri994204

Chaudhary, K., Scanlon, B., Scheffer, N., & Walden, S. (2009). *Review of the State of Art: Ground Water Under the Direct Influence of Surface Water Programs*. Bureau of Economic Geology, Jackson School of Geosciences, University of Texas at Austin, Austin, TX. https://www.beg.utexas.edu/files/content/beg/research/swr/GWUDI-Final-Report.pdf

Chin, D. A., & Qi, X. (2000). Ground water under direct influence of surface water. *Journal of Environmental Engineering (New York, N.Y.)*, *126*(6), 501–508. https://doi.org/10.1061/(ASCE)0733-9372(2000)126:6(501)

Chow, R., Frind, M. E., Frind, E. O., Jones, J. P., Sousa, M. R., Rudolph, D. L., Molson, J. W., & Nowak, W. (2016). Delineating baseflow contribution areas for streams – A model and methods comparison. *Journal of Contaminant Hydrology*, *195*, 11–22. https://doi.org/10.1016/j.jconhyd.2016.11.001

Core 6 Environmental. (2020). *Supplemental Phase II & Phase III Environmental Site Assessment, Carmacks Highway Maintenance Camp.* [Unpublished report]

Cronmiller, D. C., McParland, D. J., Goguen, K. M., & McKillop, R. J. (2020). *Carmacks surficial geology and community hazard susceptibility mapping.* Yukon Geological Survey. https://ygsftp.gov.yk.ca/publications/miscellaneous/MR20/MR20.pdf

Daus, A. D., Frind, E. O., & Sudicky, E. A. (1985). Comparative error analysis in finite element formulations of the advection-dispersion equation. *Advances in Water Resources*, *8*(2), 86–95. https://doi.org/10.1016/0309-1708(85)90005-3

Derx, J., Blaschke, A. P., Farnleitner, A. H., Pang, L., Bloeschl, G., & Schijven, J. F. (2013). Effects of fluctuations in river water level on virus removal by bank filtration and aquifer passage – A scenario analysis. *Journal of Contaminant Hydrology*, *147*, 34–44. https://doi.org/10.1016/j.jconhyd.2013.01.001

Diersch, H.-J. G. (2014). *FEFLOW Finite Element Modeling of Flow, Mass and Heat Transport in Porous and Fractured Media* (1st ed. 2014.). Springer Berlin Heidelberg. https://doi.org/10.1007/978-3-642-38739-5

Dong, Y., Xu, H., & Li, G. (2013). Wellhead protection area delineation using multiple methods; a case study in Beijing. *Environmental Earth Sciences*, *70*(1), 481–488. https://doi.org/10.1007/s12665-013-2411-2

Duncan, D., Pederson, D. T., Shepherd, T. R., & Can, J. D. (1991). Atrazine used as a tracer of induced recharge. *Ground Water Monitoring & Remediation*, *11*(4), 144–150. https://doi.org/10.1111/j.1745-6592.1991.tb00402.x

Eberhardt, C., & Grathwohl, P. (2002). Time scales of organic contaminant dissolution from complex source zones; coal tar pools vs. blobs. *Journal of Contaminant Hydrology*, *59*(1-2), 45–66. https://doi.org/10.1016/S0169-7722(02)00075-X

Environment and Climate Change Canada. (2023, May 15). *Daily Data Report for January 2021.* https://climate.weather.gc.ca/climate_data/daily_data_e.html?hlyRange=2000-04-18%7C2023-07-09&dlyRange=1999-09-01%7C2023-07-08&mlyRange=%7C&StationID=27950&Prov=YT&urlExtension=_e.html&searchType=stnProv&optLimit=yearRange&StartYear=1840&EndYear=2023&selRowPerPage=25&Line=22&lstProvince=YT&timeframe=2&Day=9&Year=2021&Month=1#

Erwin, Kate. (2023, April 12). *Precautionary boil water advisory lifted for residents of the Village of Carmacks and Little Salmon Carmacks First Nation with private wells.* Government of Yukon. https://yukon.ca/en/news/precautionary-boil-water-advisory-lifted-residents-village-carmacks-and-little-salmon-carmacks

Esri. (2023). *ESRI Gray (light)* [Base map]. http://services.arcgisonline.com/ArcGIS/rest/services/Canvas/World_Light_Gray_Base/MapServer/tile/%7Bz%7D/%7By%7D/%7Bx%7D

Fetter, C. W. (2001). *Applied hydrogeology* (4th ed.). Prentice Hall.

Focazio, M. J., Reilly, T. E., Rupert, M. G., & Helsel, D. R. (2002). *Assessing ground-water vulnerability to contamination: Providing scientifically defensible information for decision makers*. U.S. Geological Survey. https://doi.org/10.3133/cir1224

Freeze, R. A., & Cherry, J. A. (1979). *Groundwater*. Prentice-hall.

Frind, E. O., Molson, J. W., & Rudolph, D. L. (2006). Well vulnerability: A quantitative approach for source water protection. *Ground Water*, *44*(5), 732–742. https://doi.org/10.1111/j.1745-6584.2006.00230.x

Frind, E. O., Muhammad, D. S., & Molson, J. W. (2002). Delineation of three-dimensional well capture zones for complex multi-aquifer systems. *Ground Water*, *40*(6), 586–598. https://doi.org/10.1111/j.1745-6584.2002.tb02545.x

Golder Associates. (2021). *Aquifer Mapping Report: Village of Carmacks.* https://emrlibrary.gov.yk.ca/environment/aquifer-mapping-village-of-carmacks-yukon-2021.pdf

Google. (2015). *Google satellite map data* [satellite map]. Accessed within QGIS 3.22.9 software.

Government of Yukon. (2019). *Government of Yukon Lidar collection* [Ground surface elevation data]. https://maps.mcelhanney.com/Vertisee/YukonGovLidar/

Government of Yukon. (2022a, June 10). *Yukon Hydrometric Conditions Report.* https://yukon.ca/sites/yukon.ca/files/20220610-hydrometric-conditions-report.pdf

Government of Yukon. (2022b). *Contours - 50k - Canvec* [topographic map]. Geomatics Yukon. https://yukon.maps.arcgis.com/home/item.html?id=c37de6eb6c74438a82a5242ec0ba2e9c

Government of Yukon. (n.d.). *Water well registry* [interactive map]. Retrieved April 26, 2023, from https://yukon.maps.arcgis.com/apps/webappviewer/index.html?id=51322dfb133d42c4ad184fee9986048b

Henney, Samantha. (2022, December 23). *Residents of Carmacks with private wells under precautionary boil water advisory.* Government of Yukon. https://yukon.ca/en/news/residents-carmacks-private-wells-under-precautionary-boil-water-advisory

Hwang, H.-T., Park, Y.-J., Sudicky, E. A., & Forsyth, P. A. (2014). A parallel computational framework to solve flow and transport in integrated surface–subsurface hydrologic systems. *Environmental Modelling & Software: with Environment Data News*, *61*, 39–58. https://doi.org/10.1016/j.envsoft.2014.06.024

Liggett, J. E., & Talwar, S. (2009). Groundwater vulnerability assessments and integrated water resource management. *Streamline Watershed Management Bulletin*, *13*(1), 18-29.

McLaren, R. G. (2011). *GRID BUILDER, A pre-processor for 2-D, triangular element, finite-element programs* (Version 35) [Manual]. Groundwater Simulation Group, University of Waterloo, Canada.

Morrison Hershfield. (2020). *Source Water Protection Plan Little Salmon Carmacks FN Water Treatment Plant.* [Unpublished report]

Ontario Ministry of the Environment, Conservation, and Parks. (2016, November 14). *Guide for applying for drinking water works permit amendments, licence amendments.* https://www.ontario.ca/page/guide-applying-drinking-water-works-permit-amendments-licence-amendments

OpenStreetMap. (2023). *OpenStreetMap Standard* [Base map]. https://www.openstreetmap.org/copyright

Rayne, T. W., Bradbury, K. R., & Zheng, C. (2014). Correct delineation of capture zones using particle tracking under transient conditions. *Ground Water*, *52*(3), 332–334. https://doi.org/10.1111/gwat.12141

Schilling, O. S., Park, Y.-J., Therrien, R., & Nagare, R. M. (2019). Integrated surface and subsurface hydrological modeling with snowmelt and pore water freeze-thaw. *Ground Water*, *57*(1), 63–74. https://doi.org/10.1111/gwat.12841

Statistics Canada. (2021, Aug 17). *Population served by drinking water plants (Table 38-10-0093-01)*. https://doi.org/10.25318/3810009301-eng

Tecplot Inc. (2022). *Tecplot 360 EX User's Manual* (Version 14403) [Manual]. Tecplot Inc. https://tecplot.azureedge.net/products/360/current/360_users_manual.pdf

Tetra Tech. (2017a). *City of Dawson Aquifer and Wellhead Protection Plan.* http://cityofdawson.ca/Home/DownloadDocument?docId=a7a69d70-4f6f-4c7e-ab84-d0de8c2b7516

Tetra Tech. (2017b). *Overarching Yukon source water supply and protection study - Summary report.* https://yukon.ca/sites/yukon.ca/files/env/env-overarching-yukon-source-water-supply-protection-study-summary-report.pdf

Todd, D. K., & Mays, L. W. (2005). *Groundwater hydrology* (3rd ed.). Wiley.

Turcotte, B. (2021). Flooding processes and recent trends in ice-induced high-water levels along rivers of Northwestern Canada. In *21st Workshop on the Hydraulics of Ice, Saskatoon, SK, CGU HS Committee on River Ice Processes and the Environment*. http://www.cripe.ca/docs/proceedings/21/Turcotte-2021.pdf

Vassolo, S., Kinzelbach, W., & Schaefer, W. (1998). Determination of a well head protection zone by stochastic inverse modelling. *Journal of Hydrology (Amsterdam)*, *206*(3-4), 268–280. https://doi.org/10.1016/S0022-1694(98)00102-4

Vrba, J., & Zoporozec, A. (1994). *Guidebook on mapping groundwater vulnerability*. Heise.

Water Survey of Canada. (2023a, March 2). *Daily discharge graph for Yukon River at Carmacks (09AH001).* https://wateroffice.ec.gc.ca/report/historical_e.html?stn=09AH001&dataType=Daily%C2%B6meterType=Level&year=2019&mode=Graph&start_year=1850&end_year=2023&page=historical

Water Survey of Canada. (2023b, March 2). *Real-time hydrometric data graph for Nordenskiold River below Rowlinson Creek (09AH004).* https://wateroffice.ec.gc.ca/report/real_time_e.html?stn=09AH004

Wiebe, A. J., Rudolph, D. L., Pasha, E., Brook, J. M., Christie, M., & Menkveld, P. G. (2021). Impacts of event-based recharge on the vulnerability of public supply wells. *Sustainability (Basel, Switzerland)*, *13*(14), 7695. https://doi.org/10.3390/su13147695

Winter, T. C., Harvey, J. W., Franke, O. L., & Alley, W. M. (1998). *Ground water and surface water; a single resource.* U.S. Geological Survey. https://doi.org/10.3133/cir1139

Woessner, W. W. (2000). Stream and fluvial plain ground water interactions: Rescaling hydrogeologic thought. *Ground Water*, *38*(3), 423–429. https://doi.org/10.1111/j.1745-6584.2000.tb00228.x

Yuan, W., Liu, S., Liang, S., Tan, Z., Liu, H., & Young, C. (2012). Estimations of evapotranspiration and water balance with uncertainty over the Yukon River Basin. *Water Resources Management*, *26*(8), 2147–2157. https://doi.org/10.1007/s11269-012-0007-3

Yukon Geological Survey. (2022). *Yukon digital bedrock geology*. https://data.geology.gov.yk.ca/Compilation/3